Quaternary Science Reviews 299 (2023) 107878

Contents lists available at ScienceDirect

Quaternary Science Reviews

journal homepage: www.elsevier.com/locate/quascirev

Relict permafrost preserves megafauna, insects, pollen, soils and pore-ice isotopes of the mammoth steppe and its collapse in central Yukon

Alistair J. Monteath [a, *], Svetlana Kuzmina [a, b], Matthew Mahony [a], Fabrice Calmels [c], Trevor Porter [d], Rolf Mathewes [e], Paul Sanborn [f], Grant Zazula [g], Beth Shapiro [h], Tyler J. Murchie [i], Hendrik N. Poinar [i], Tara Sadoway [j], Elizabeth Hall [g], Susan Hewitson [g], Duane Froese [a, **]

[a] Department of Earth and Atmospheric Sciences, University of Alberta, Edmonton, Canada
[b] Borissiak Paleontological Institute, Russian Academy of Sciences, Moscow, Russia
[c] Yukon Research Centre, Yukon University, Whitehorse, Canada
[d] Department of Geography, Geomatics and Environment, University of Toronto - Mississauga, Canada
[e] Department of Biological Sciences, Simon Fraser University, British Columbia, Canada
[f] Ecosystem Science and Management Program, University of Northern British Columbia, Prince George, Canada
[g] Yukon Palaeontology Program, Government of Yukon, Whitehorse, Canada
[h] Department of Ecology and Evolutionary Biology, University of California Santa Cruz, USA
[i] McMaster Ancient DNA Centre, McMaster University, Hamilton, Canada
[j] The Hospital for Sick Children, Toronto, Canada

ARTICLE INFO

Article history:
Received 25 July 2022
Received in revised form
15 November 2022
Accepted 16 November 2022
Available online 29 November 2022

Handling Editor: Dr Donatella Magri

Keywords:
Pleistocene
Paleoclimatology
North America
Sedimentology
Loess
Mammoth steppe
Steppe-tundra
Beringia
Pleistocene-holocene transition
Palaeoecology

ABSTRACT

In eastern Beringia (unglaciated Alaska and western Yukon), the Pleistocene-Holocene transition was characterised by rapid changes in plant, insect and mammal communities as the mammoth steppe ecosystem was replaced, first by shrub tundra and later boreal forest. These changes indicate a transition from well drained terrain with deep active layers to wetter, cooler soils, to which steppe-tundra vegetation was poorly adapted. The nature and precise timing of these events is not well resolved, particularly in central Yukon where regional climate may have been strongly affected by the retreating Cordilleran-Laurentide ice sheet complex. Resolving this uncertainty is not only important for understanding past ecosystems, but also provides a long-term perspective for contemporary environmental change and shrub expansion that affects large areas of northern high-latitudes today. Here, we report chronology (41 radiocarbon dates), stratigraphy, pore-ice $\delta^2H/\delta^{18}O$ measurements, pollen data, megafauna remains and fossil insect assemblages from a permafrost-preserved loessal sequence in central Yukon, named Lucky Lady. The site spans the interval from ca. 17,000 to 8000 cal yr BP (calibrated years before C.E. 1950) and records the Pleistocene-Holocene transition in exceptional resolution. Full glacial environments (ca. 16,500 cal yr BP) supported elements of steppe-tundra vegetation and an insect fauna dominated by *Connatichela artemisiae* - an endemic weevil indicating warm soil temperatures. The collapse of the mammoth steppe ecosystem began with slowing of loess accumulation and development of paleosol ca. 13,480 cal yr BP. At this time, *C. artemisiae* remains become infrequent and *Artemisia* pollen decline to be replaced by Cyperaceae (ca. 13,220), before mesic, shrub taxa (likely dwarf *Betula* and *Salix*) becomes dominant ca. 13,210 cal yr BP. The establishment of shrub tundra is associated with rapid changes in $\delta^2H/\delta^{18}O$ measurements, suggesting that ecological turnover coincided with a shift in atmospheric conditions and moisture availability. Finally, boreal vegetation communities became established ca. 10,680 cal yr BP. The replacement of steppe-tundra vegetation in central Yukon lagged other areas of eastern Beringia by as much as 1000 years and coincided with rapid deglaciation during the Bølling–Allerød time-period (14,600–12,900 cal yr BP). Turnover in insect and vegetation communities took place in ca. 40 years

* Corresponding author.
** Corresponding author.
E-mail addresses: ali.monteath@ualberta.ca (A.J. Monteath), duane@ualberta.ca (D. Froese).

https://doi.org/10.1016/j.quascirev.2022.107878

as shrub tundra became dominant. This rapid turnover has parallels with contemporary Arctic greening and re-emphasises the sensitivity of high-latitude environments to climate change.

1. Introduction

Eastern Beringia (Alaska and western Yukon) includes the northwestern region of North America that remained largely unglaciated throughout the Pleistocene. It is a special place scientifically as it represents, conceptually, both a glacial refugium, periodically separated from continental North America by the Cordilleran and Laurentide Ice sheets (Hultén, 1937; Hopkins, 1982; Heintzman et al., 2016), while at the same time an extension of a northern Holarctic closely connected with eastern Asia during Pleistocene cold stages (e.g. Guthrie, 1990a; Froese et al., 2017; Vershinina et al., 2021). Throughout the late Pleistocene the landscape was home to a variety of extinct and extant grazing megafauna (animals >44 kg), including; horse (*Equus* spp.), steppe-bison (*Bison priscus*) and woolly mammoth (*Mammuthus primigenius*), part of the mammoth steppe ecosystem rooted in a cold adapted and precipitation-limited steppe-tundra flora (Guthrie, 1982). Dry soils and deep active layer depths supported a vegetation assemblage with no modern analog, dominated by grasses, sedges, *Artemisia* and a range of other forbs (Schweger, 1982; Goetcheus and Birks, 2001; Zazula et al., 2003; Willerslev et al., 2014).

The mammoth steppe ecosystem collapsed at the end of the Pleistocene (ca. 14,000 cal yr BP) as increasing effective moisture (precipitation minus evaporation) led to paludification, cooler soil conditions and shallower active layers that favoured the expansion of woody shrub taxa including *Betula* and *Salix* (Guthrie, 2001; Mann et al., 2013, 2015). These new conditions were largely inhospitable to both grazing megafauna, which relied upon the steppe-tundra vegetation, and burrowing mammals, such as the arctic ground squirrel (*Urocitellys parryii*), that require deep active layer depths (>0.9 m) for nest construction and hibernation (Guthrie, 1984, 2001; Zazula et al., 2005). In eastern Beringia, lake-sediments provide the most common continuous palaeoecological records that span the transition from steppe-tundra to shrub tundra vegetation. These records, however, are heavily reliant on pollen data, which can rarely be identified to species level, and are often founded on chronology based on unreliable aquatic or bulk-sediment radiocarbon dates (Abbott and Stafford, 1996; Anderson et al., 2003). Therefore, detailed environmental information, such as soil temperatures and active-layer depths, as well as the precise chronology and climate controls of late Pleistocene vegetation turnover, remain unclear. Resolving these uncertainties is important for understanding past environmental change, late Quaternary extinction events and the conditions encountered by early human communities (Edwards et al., 2005; Guthrie, 2006; Potter et al., 2017). Many of these questions also have implications for understanding modern climate-driven vegetation change and geo-engineering proposals, such as the "rewilding" of the Arctic (Myers-Smith et al., 2011; Zimov, 2005).

In this study, we focus on an exceptional site from the Klondike region of central Yukon named Lucky Lady (Fig. 1). This north-facing exposure is formed of permafrost-preserved loessal (yedoma) deposits that accumulated rapidly through the late Pleistocene and Early-Mid Holocene. The high-resolution, continuous record preserves a range of palaeoenvironmental evidence including diverse fossil beetle (Coleoptera) assemblages and the stable isotopes ($\delta^2H/\delta^{18}O$) of syngenetic pore-ice, representing paleo-meteoric waters. Beetle fauna are sensitive to a range of narrow environmental conditions (e.g. soil temperature) and respond quickly to changes in vegetation and climate (Sher and Kuzmina, 2007). Remains can be identifiable to species level and some taxa are known to only inhabit specific plants or vegetation, making them important palaeoecological proxies for past ecosystems. One limitation of this approach, however, is that large quantities of sediment, often >10 kg or more, are needed to retrieve representative samples. Because of this, in eastern Beringia beetle remains are typically sampled from non-continuous sections and so only provide snapshots of past environments (Matthews, 1974; Elias, 2000; Zazula et al., 2006; Kuzmina et al., 2008). The rapidly accumulating sediments and abundance of dateable (radiocarbon) terrestrial macrofossils at Lucky Lady allow changes in fossil beetle assemblages to be examined at near decadal resolution in some places. Outside glaciated regions, syngenetic pore ice provides a unique opportunity to directly measure changes in precipitation isotopes through time and represents an emerging proxy in the palaeo-sciences (Porter and Opel, 2020). The Lucky Lady pore-ice $\delta^2H/\delta^{18}O$ record is only the second high-resolution ground ice time-series in northern Canada to be developed for hydroclimate reconstruction. We couple these palaeoecological and pore-ice $\delta^2H/\delta^{18}O$ data with stratigraphic observations, pollen counts and published eDNA analyses (Murchie et al., 2021a, 2021b) to develop a detailed, multi-proxy record of environmental change in central Yukon, spanning the collapse of the mammoth steppe ecosystem.

2. Materials and methods

2.1. Site description

The Lucky Lady site is located 46 km south of Dawson City in the Klondike Placer District of central Yukon. The site lies near the middle of a broad valley on lower Sulphur Creek, opposite the mouth of Brimstone Gulch (Fig. 1). Placer gold mining has allowed access for more than a decade and several exposures were present over multiple years of study. These were sampled with respect to a prominent paleosol in Unit 1 that provides an isochron across the site (Fig. 5a) (see stratigraphic description below). Samples for insect and pollen analyses were collected between 2008 and 2010, while pedological descriptions were made in 2009. Pore-ice δ^2H and $\delta^{18}O$ measurements were made on five vertical cores taken in subsequent years (cores LL12, LLA, LLB, LLC, and LLS). These were drilled with reference to the prominent paleosol in Unit 1 and dated independently.

The 11.5 m exposed section consists of sandy silts and loess, sourced from within the catchment, that accumulated throughout the late Pleistocene and Early Holocene, after the site became an alluvial terrace (Fig. 2). The final ~1 m of the sequence is formed of peat and organic rich soils that are distinct from the rest of the sequence. Deposits at Lucky Lady can be divided into two depositional units: Unit 1 consists of 3.5 m of grey sandy-silt with *in situ* graminoid vegetation and arctic ground squirrel nests. Near the top of this unit a prominent paleosol (4–10 cm thick) can be traced laterally for hundreds of metres around the exposure. Cryostratigraphy is characterised by thin (1–3 mm), parallel, wavy lenticular cryostructures in otherwise structureless sediment. One thin ice

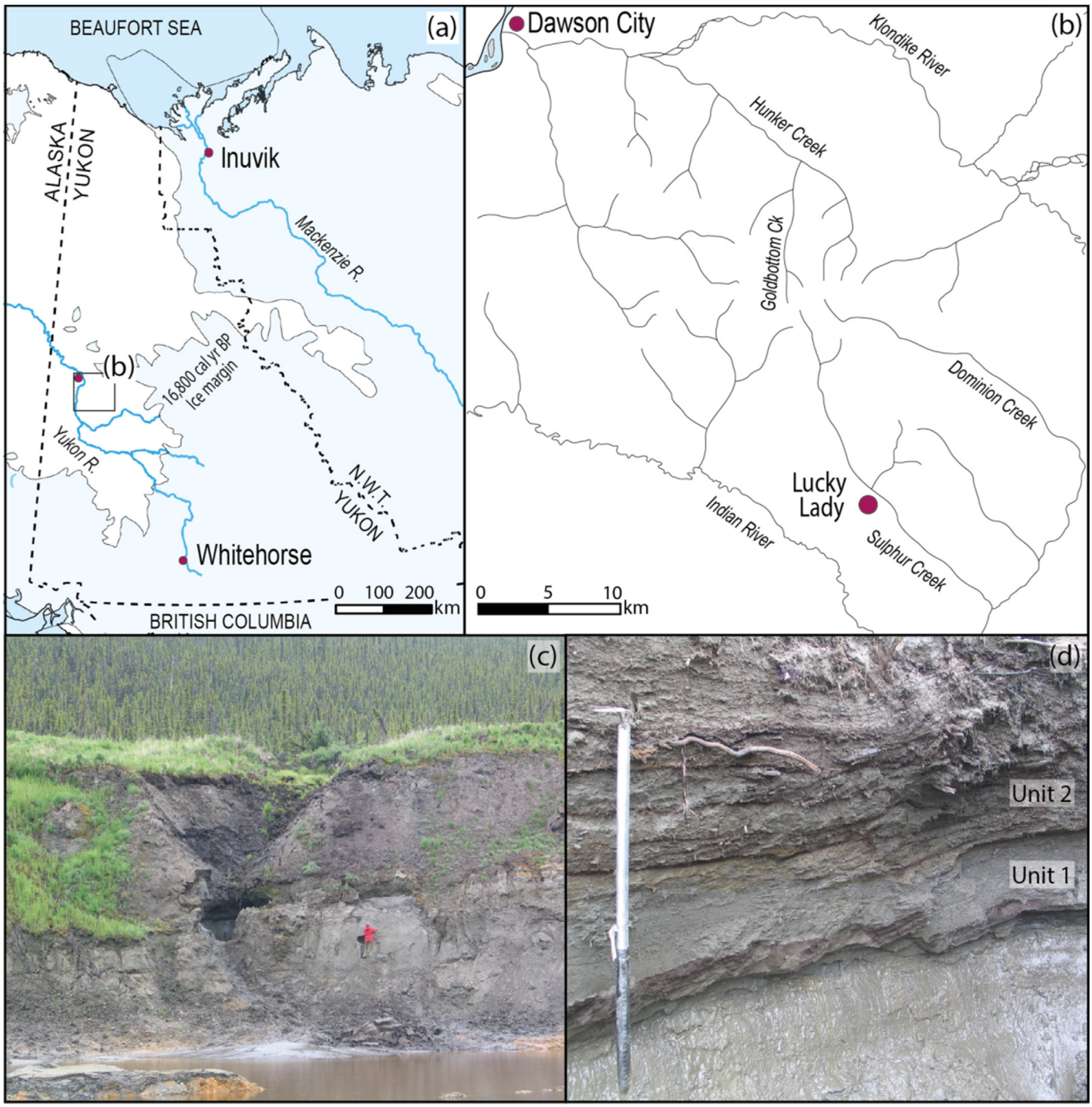

Fig. 1. (a) Map of the study area and location of the Klondike in Yukon, Canada. Ice margins plotting using GIS data from Dalton et al. (2020). (c) The location of the Lucky Lady placer mine in Klondike. (c) Photograph of the Lucky Lady exposure. (d) Photograph of the Unit 1/Unit 2 transition (ice-pick shown in the left of the figure provides scale).

wedge (~30 cm wide) cross-cuts the paleosol and is truncated beneath the Unit 1/Unit 2 boundary. Unit 2 is separated from Unit 1 by a sharp contact and includes ~8 m of organic-rich grey and black silt, with *in situ* shrub vegetation, that extends to the top of the exposure. The sediment in Unit 2 generally becomes more organic-rich with height and includes *in situ* tree stumps and black organic horizons/laterally discontinuous paleosols (Fig. 2), separated by lenses of grey silt. No ice wedges are present in Unit 2. Cryostructures are mainly parallel lenticular (~2 mm thick) and microlenticular to structureless.

2.2. Stratigraphy and soils

The Lucky Lady site was examined several times over multiple years as continued placer mining allowed new access. Stratigraphic sections were surveyed for cryostratigraphy, and paleoecological indicators. Lateral permafrost cores were collected from exposures using a 3 inch diameter coring bit, powered by a gas-powered drill. Elevations of these samples were measured with a laser range finder (Lasertech 200XL) with 0.1 m vertical precision. Vertical cores were taken using a 4 inch diameter core with a drill system

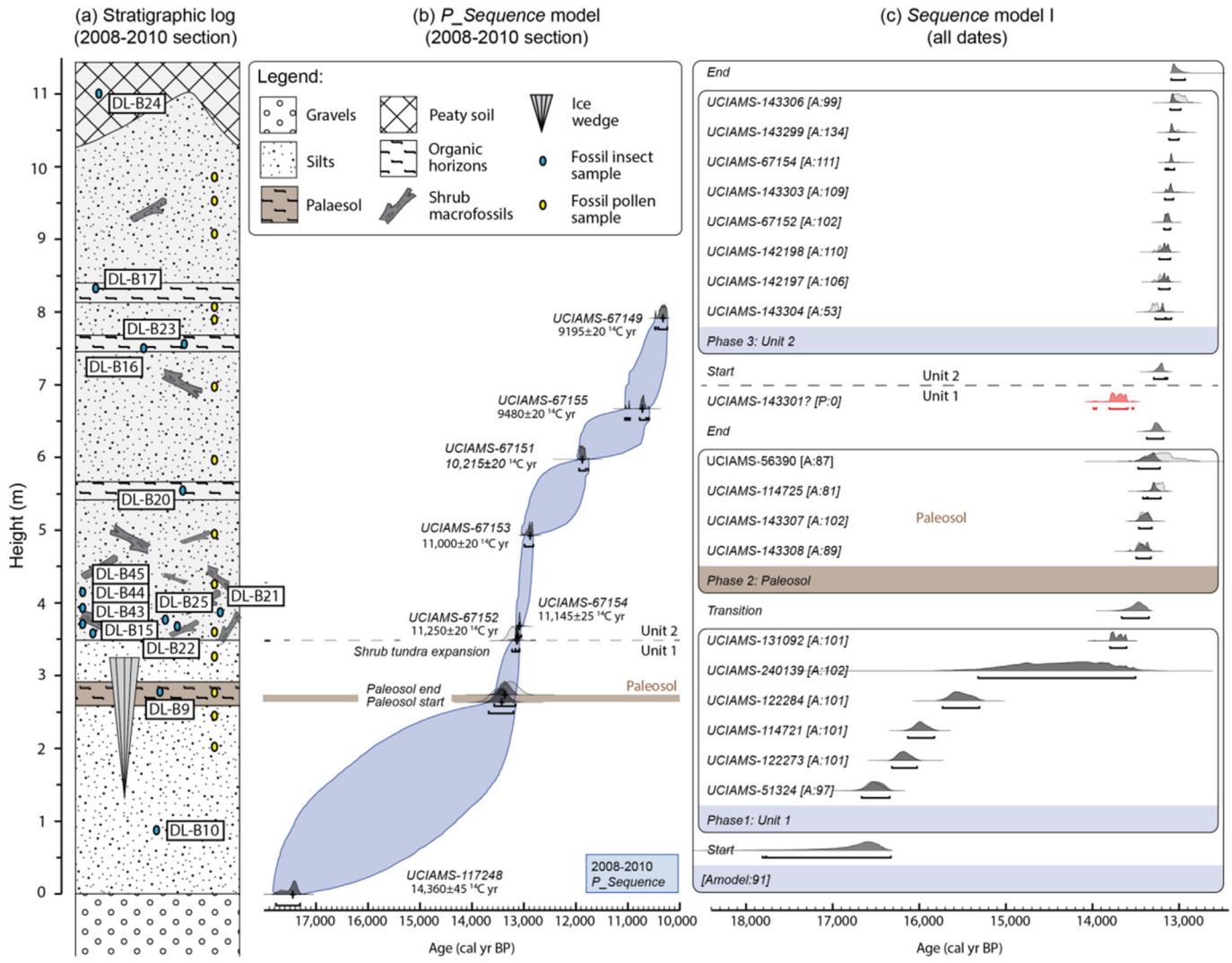

Fig. 2. Stratigraphy and chronology from the Lucky Lady exposure sampled and described in 2008–2010. (a) Stratigraphy of the Lucky Lady section as described in 2009. (b) The 2008–2010 *P_Sequence* age-depth model plotted on the same depth scale as the stratigraphic log. (c) The *Sequence* age-depth model used to constrain the timing of paleosol formation and the Unit 1/Unit 2 transition at Lucky Lady. One outlier radiocarbon date is shown in red and was excluded from the *Sequence* model. Note that additional labels/colouring on the *Sequence* model output do not affect the model functioning and are only added to guide the reader. (For interpretation of the references to colour in this figure legend, the reader is referred to the Web version of this article.)

similar to Calmels et al. (2005) and Calmels and Froese (2009). All samples were shipped frozen to the Permafrost Archive Science Laboratory (PACS), University of Alberta, Canada, and stored at −25 °C.

A pedological description of the section exposed in 2009 was recorded (Table 3), and soil horizon samples were analysed for particle size distribution by the pipette method (Kroetsch and Wang, 2008), and carbon content by the combustion method (Skjemstad and Baldock, 2008). The latter analysis was done on paired subsamples with and without removal of carbonates by HCl in order to allow separation of organic and inorganic carbon. Full results are reported in Table S1.

2.3. Radiocarbon dating

We prepared 33 samples from herbaceous plant remains, twigs, arctic ground squirrel middens, shrubs, leaves and conifer needles for radiocarbon dating using established acid-base-acid methodology (e.g. Reyes et al., 2010) (Table 1). All samples were pre-treated at the University of Alberta alongside sub-samples of comparable mass from two secondary standards: (1) AVR-PAL-07, an internal standard of last interglacial age to establish background radiocarbon abundance (MartinezDe La Torre et al., 2019), and (2) FIRI-F, a well dated international standard, to verify age quality. Pretreatment of all samples followed standard acid-base-acid procedures. Briefly, solutions were heated to 70 °C, submerged in 1 M HCl for 30 min and then 1 M NaOH for 60 min, with the solution changed until clear. This was followed by a second application of 1 M HCl for 30 min and finally rinses with ultrapure water until neutral. Collagen was extracted from eight megafauna samples (Table 2) using ultrafiltration at the Keck-Carbon Cycle accelerator mass spectrometry (AMS) facility (UCIAMS) (Brown et al., 1988). CO_2 production, graphitization and measurement of radiocarbon abundance of all samples were completed at UCIAMS.

2.4. Bayesian age modelling

We developed multiple age models from different sampling transects/vertical cores to establish the chronology of the Lucky Lady site. All of these were constructed using the Bayesian

Table 1
Radiocarbon (^{14}C) dates from the Lucky Lady site ordered by section/vertical core. Dates were calibrated using OxCal version 4.4 (Bronk Ramsey, 2009b) and the Intcal20 calibration curve (Reimer et al., 2020). Calibrated age ranges are reported at 2σ uncertainty. The weights of small mass radiocarbon samples that typically have lower precision are indicated. DF sample numbers refer to the year of sampling (2008, 2012 and 2013).

Sample ID	Height in section (m)	Lab ID	^{14}C date	Age (cal. BP)	Median (cal. BP)	Mass (mgC)	Material
DF08-58	>9.5	UCIAMS-51321	1475 ± 20	1385–1309	1353	–	plant macrofossil
DF08-56	8.0	UCIAMS-51319	8875 ± 20	10,160–9895	10,024	–	twig
DF08-57	6.5	UCIAMS-51320	8800 ± 20	10,110–9690	9816	–	birch root
DF08-26 A	2.7	UCIAMS-56390	11,290 ± 160	13,446–12809	13,151	0.052	twigs/graminoid
DF12-18	2.7	UCIAMS-114725	11,360 ± 40	13,293–13108	13,203	0.16	twigs/graminoid
DF12-18	2.7	UCIAMS-143307	11,535 ± 35	13,454–13291	13,375	–	twigs/graminoid
DF12-18	2.7	UCIAMS-143308	11,580 ± 35	13,482–13312	13,415	–	twigs/graminoid
DF13-05	1.7	UCIAMS-131092	11,875 ± 35	13,769–13576	13,678	–	ground squirrel nest
DF12-61 b	0.4	UCIAMS-114721	13,300 ± 30	16,157–15818	15,995	–	ground squirrel nest
DF08-97	0	UCIAMS-51324	13,680 ± 35	16,726–16295	16,494	–	ground squirrel nest
LL2-12-170-6	1.84	UCIAMS-240139	12,200 ± 340	15,389–13499	14,337	0.25	twig
LL2-12-184	1.7	UCIAMS-122284	12,980 ± 60	15,756–15285	15,521	0.19	graminoid
LL2-12-259	0.95	UCIAMS-122273	13,430 ± 35	16,316–15993	16,159	–	graminoid
LL2A-17	7.36	UCIAMS-143297	9300 ± 25	10,575–10420	10,511	–	leaves/twigs
LL2A-154	5.99	UCIAMS-143298	10,020 ± 170	12,375–11147	11,598	0.044	twigs
LL2A-308	4.45	UCIAMS-143299	11,125 ± 30	13,090–12896	13,021	–	twigs
LL2A-425	3.28	UCIAMS-143301	11,870 ± 50	13,775–13565	13,673	0.21	twig
LL2B-25	5.7	UCIAMS-143302	10,340 ± 45	12,391–12003	12,191	0.18	twig
LL2B-155	4.4	UCIAMS-143303	11,165 ± 35	13,111–12973	13,048	–	twigs/graminoid
LL2B-225	3.7	UCIAMS-143304	11,405 ± 30	13,313–13153	13,244	–	twigs/graminoid
LL2C-37	4.3	UCIAMS-143306	11,070 ± 30	13,047–12816	12,940	–	twigs/graminoid
LL2C-88(2)	3.58	UCIAMS-142198	11,290 ± 40	13,235–13065	13,137	–	shrub/twigs
LL2C-88	3.58	UCIAMS-142197	11,300 ± 35	13,238–13070	13,144	–	shrub/twigs
LL2S-169	10.47	UCIAMS-143296	7750 ± 25	8590–8454	8532	–	twigs
LL2S-189	10.27	UCIAMS-142212	7975 ± 25	8992–8725	8870	–	needle/leaves
LL2S-353	8.63	UCIAMS-142211	8770 ± 30	9907–9634	9770	–	leaves/twigs
LLII-7.5(+)	10.2	UCIAMS-67150	2415 ± 15	2607–2356	2419	–	plant macrofossil
LLII-5.25(+)	7.95	UCIAMS-67149	9195 ± 20	10,476–10254	10,339	–	shrub/twigs
LLII-4.0(+)	6.7	UCIAMS-67155	9480 ± 20	10,990–10609	10,721	–	shrub/twigs
LLII-2.8(+)	5.5	UCIAMS-67151	10,215 ± 20	11,946–11817	11,885		plant macrofossil
LLII-2.25(+)	4.95	UCIAMS-67153	11,000 ± 20	12,968–12740	12,842	–	shrub/twigs
LLII-1.0(+)	3.7	UCIAMS-67154	11,145 ± 25	13,093–12978	13,038	–	shrub/twigs
LLII-0.81(+)	3.51	UCIAMS-67152	11,250 ± 20	13,148–13061	13,103	–	shrub/twigs

Table 2
Megafauna fossils collected from the Lucky Lady site. Dates were calibrated using OxCal version 4.4 (Bronk Ramsey, 2009b) and the Intcal20 calibration curve (Reimer et al., 2020). Calibrated age ranges are reported at 2σ uncertainty.

n.	Sample ID	Mammal	Element	Lab ID	^{14}C date	Age (cal. BP)	Median (cal. BP)
1	YG 427.1	*Bison priscus*	Cervical vertebra	UCIAMS-264371	12,325 ± 35	14,811–14110	14,283
2	YG 427.7	*Bison priscus*	2nd phalanx, complete	UCIAMS-264372	12,340 ± 35	14,819–14140	14,335
3	YG 427.8	*Bison priscus*	Cervical vertebra fragment	–	–	–	–
4	YG 427.9	*Bison priscus*	Lumbar vertebra	–	–	–	–
5	YG 427.10	*Bison priscus*	Horn sheath fragment	–	–	–	–
6	YG 427.12	*Bison priscus*	Cranial fragment	–	–	–	–
7	YG 427.11	*Bison priscus*	Cervical vertebra fragments	UCIAMS-264370	12,410 ± 25	14,845–14281	14,496
8	YG 427.2	–	Bone fragment (undiff.)	–	–	–	–
9	YG 427.3	–	Bone fragment (undiff.)	–	–	–	–
10	YG 427.4	–	Bone fragment (undiff.)	–	–	–	–
11	YG 427.6	–	Bone fragment (undiff.)	–	–	–	–
12	YG 427.5	*Rangifer*	Scapula fragment, left	UCIAMS-264369	1540 ± 15	1511–1365	1399
13	YG 428.1	*Equus* spp.	Femur, near complete, right	UCIAMS-117248	14,360 ± 45	17,784–17325	17,470
14	YG 428.2	*Equus* spp.	Humerus, complete, right	UCIAMS 117249	14,165 ± 45	17,367–17075	17,215
15	YG 428.3	*Equus* spp.	Mandible fragment, right	UCIAMS-117250	12,280 ± 35	14,786–14078	14,198
16	YG 428.4	*Equus* spp.	1st phalanx, complete	UCIAMS-264373	12,915 ± 35	15,594–15286	15,438

statistical program Oxcal v.4.4 (Bronk Ramsey, 2009a) and the Intcal20 northern hemisphere calibration curve (Reimer et al., 2020). While we expect radiocarbon dates from different exposures at the site to be broadly in agreement we cannot rule out lateral variations in sedimentation. Therefore, we took a conservative approach and only developed *P_Sequence* models (which include depth/height as a prior) from radiocarbon dates sampled in carefully measured transects or vertically drilled cores.

Firstly, we ran a *Sequence* model (hereafter *Sequence* model I) to constrain the timing of key stratigraphic changes (timing of the prominent paleosol and the Unit 1/Unit 2 transition) and take advantage of the large number of radiocarbon dates from different exposures across the Lucky Lady site (Bronk Ramsey, 2009a) (Fig. 2c). This model includes three *Phases* with no defined internal order (stratigraphic or temporal). The first two *Phases* are continuous, while the third is sequential as an unknown period of accumulation took place between *Phase* two and *Phase* three. *Phase* one includes six radiocarbon dates from beneath the laterally continuous paleosol that is evident across the Lucky Lady site. *Phase* two includes four radiocarbon dates from the paleosol itself, and *Phase*

Table 3
Pedological description of soil horizons surrounding the prominent paleosol and Unit 1/Unit 2 transition, as exposed in 2009. Datum is set at upper surface of prominent paleosol A horizon. The described sequence corresponds to Unit 1 and the transition to Unit 2 as shown in Fig. 5a. Soil horizon nomenclature follows Soil Classification Working Group (1998), using descriptive terminology from Day (1983). Suffixes in horizon designations indicate: b = buried; g = gleyed (affected by redox processes resulting in redistribution of iron); h = enriched in organic matter; k = primary carbonates present; y = cryoturbated; z = frozen.

Horizon (sample n.)	Height in section (cm)	Description
Ahkyzb1 (Y09-02-06)	290–260	Very dark grey (10 YR 3/1 m, 2.5Y 3/1 m) silt loam; weak fine platy; very friable; abundant, very fine roots; weakly effervescent; clear, irregular boundary; 20–40 cm thick; includes some mesic peaty material.
Ckgzl (Y09-02-01)	260–110	Very dark greyish brown (2.5Y 3/2 m) and black (2.5Y 2.5/1 m) silt; common, medium and coarse, faint dark olive brown (2.5Y 3.5/3 m) mottles; moderate, fine and medium platy; friable; few very fine roots; moderately effervescent; abrupt wavy boundary; 150–170 cm thick; darker, organic matter-enriched bands 1 mm-4 cm thick comprise 10% of total thickness.
Ahkzb (Y09-02-01)	110–100	Very dark grey (2.5Y 3/1 m) and dark grey (2.5 y 4/1 m) silt loam; weak, fine granular; friable; abundant very fine and fine roots; moderately effervescent; clear, wavy boundary 5–12 cm thick.
Ckgz2 (Y09-02-02)	100–0	Dark grey (2.5Y 4/1 m) and very dark brown (10 YR 2/2 m) silt loam; many coarse, distinct olive brown (2.5Y 4/3 m) mottles; weak, fine and medium subangular blocky; friable; plentiful, very fine and fine roots; strongly effervescent; abrupt, wavy boundary; 80–100 cm thick; includes several 1–2 cm thick Ahkbz horizons with total thickness around 10 cm, laterally continuous for >2 m).
Ahkzb2 (Y09-02-03)	0–8	Very dark brown (10 YR 2/2) and very dark greyish brown (10 YR 3/2 m) silt loam; weak, fine and subangular blocky; friable; plentiful, very fine and fine roots; weakly effervescent; clear irregular boundary; 3–11 cm thick.
Ckgz3 (Y09-02-04)	8–30	Dark olive grey (5Y 3/2 m) silt; moderate, medium platy; friable, few very fine roots; strongly effervescent; clear wavy boundary; 18–30 cm thick; perhaps palaeo-active layer; lower ice content than underlying horizon.
Ckgz4 (Y09-02-05)	30-100+	Dark olive grey (5Y 3/2 m) silt loam; massive; moderately effervescent; >50% ice content.

three includes eight radiocarbon dates from above the Unit 1/Unit 2. This age model was run with a *General_Outlier* model (Bronk Ramsey, 2009b). One low mass (0.21 mg C) radiocarbon date was removed from the model (UCIAMS-143301) as it caused a substantial age reversal (Fig. 2c). We used boundaries between *Phases* to quantify 'start' and 'end' dates of stratigraphic transitions.

Secondly, we developed a *P_Sequence* depositional model to provide chronology for insect and pollen analyses presented in this study (Bronk Ramsey, 2008). This age-depth model includes seven radiocarbon dates and follows the same transect as the insect and pollen samples - collected between 2008 and 2010. In order to include the results from the Lucky Lady *Sequence* model I we re-ran this model excluding radiocarbon dates from 2008 to 2010 sampling transect, to avoid circularity (Fig. S1) (hereafter *Sequence* model II). We then included the two sigma modelled age ranges for the *Phase* one/*Phase* two transition (the start paleosol formation; 13,665–13,345 cal yr BP), the end of *Phase* two (the end paleosol formation; 13,384–13,191 cal yr BP) and the start of *Phase* three (the transition from Unit 1 to Unit 2; 13,318–13,169 cal yr BP) in the 2008–2010 transect *P_Sequence* depositional model. Insect and pollen samples taken from outside the *P_Sequence* depositional model were approximately date by extrapolating model results. These modelled ages are in good agreement with radiocarbon dates taken from similar heights in other areas of the exposure. An exception to this is insect sample DL_24 which was approximately dated by radiocarbon dates UCIAMS-51321 and UCIAMS-67150.

Finally, we developed a *P_Sequence* depositional model for each of the five vertical cores taken at Lucky Lady (Fig. 3) (Cores LL12, LLA, LLB, LLC, and LLS). Cores LL12 and LLC were linked by the paleosol and combined as one composite model. These age-depth models included boundaries between sedimentary units where accumulation rates are likely to have changed. All *P_Sequence* depositional models presented in this study were run with a variable *k* parameter (Bronk Ramsey and Lee, 2013) and a *General_Outlier* model, where each radiocarbon date had a 5% likelihood of being a statistical outlier (Bronk Ramsey, 2009b). A radiocarbon date from the base of core LL2A (UCIAMS-143301) was identified as a possible outlier in *Sequence* model I, despite good agreement with other radiocarbon dates from core LL2A. Pore-ice $\delta^{18}O$ measurements from the base of core LL2A are enriched relative to measurements from other vertical cores with the same apparent age, supporting this interpretation.

2.5. Mammal fossils

We collected 16 mammal fossils from the Lucky Lady site between June 2010 and July 2012. These included typical members of the late Pleistocene fauna, such as horse (*Equus* spp.) and steppe-bison (*Bison priscus*), as well as caribou (*Rangifer tarandus*) and several other bone fragments that were not identified (Fig. 4). Although most specimens were collected as detrital elements in front of the section, a near complete horse right femur (YG 428.1) was recovered *in situ* at the silt-gravel contact and radiocarbon dated to ca. 17,470 cal yr BP (UCIAMS-117248) (Table 2).

2.6. Pollen samples

We processed 14 sediment samples collected between 2008 and 2010 for pollen and spore quantification at the University of Alberta. Two tablets of acetolyzed *Lycopodium* spores (batch number 483216; 18,583 mean spores) were added to each sample before processing. Following this, we immersed samples in dilute HCl, to remove carbonates, before washing and sieving the sediments to remove coarse debris. We then used heavy liquid (ZnBr) separation to isolate organics before washing the residue in HCl. Subsamples were dehydrated with glacial acetic acid and acetolyzed in a hot water bath for 5 min. After dehydration in ethanol, residues were stained red with Safranin, washed with tertiary butyl alcohol and stored in silicone oil.

Pollen analysis was mostly conducted at 400× magnification, using a Nikon Eclipse 80i microscope, with occasional use of oil immersion at 1000X to confirm identifications. Due to low concentrations, more than one slide was prepared for quantitative analysis in some samples. Pollen sums used for percentage calculations exceeded 200 in all cases (range 202–351 grains). The basic sum used for percentage calculations includes all trees and shrubs, herbs, and spores except mosses, fungi, or algae. Bryophyte and fungi percentages are calculated from the basic sum plus these constituents. Full results are reported in Supplementary Materials, Table S2.

2.7. Insect fossils

Fossil insects were recovered from 14 bulk-sediment samples collected between 2008 and 2010, including re-sampling of key

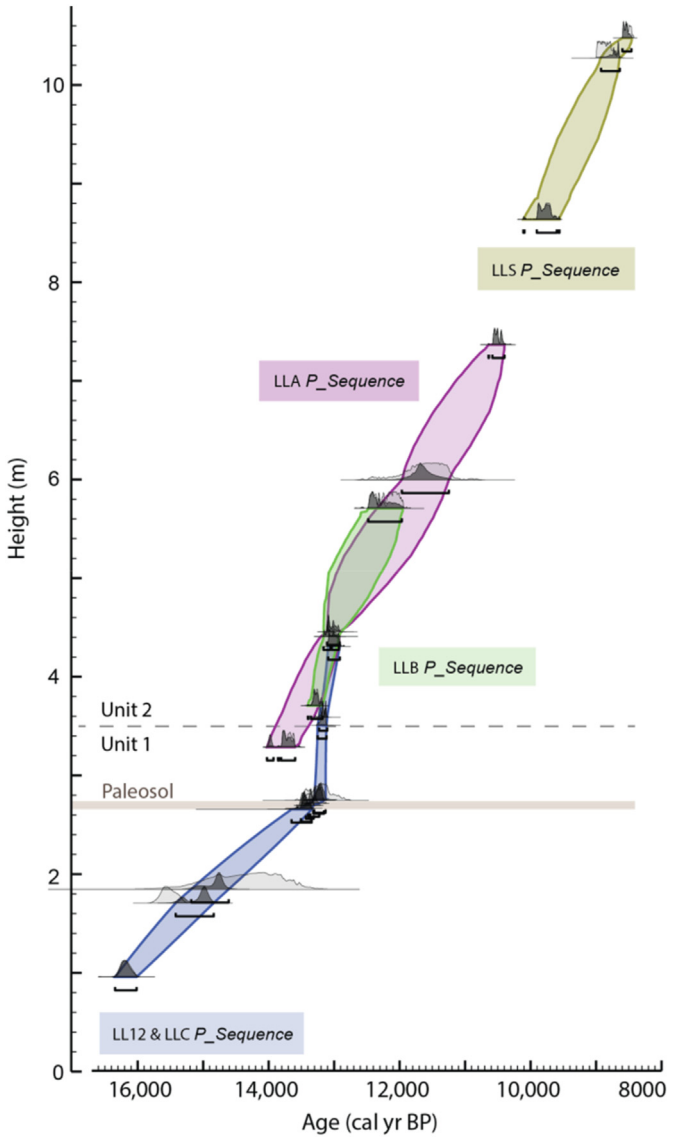

Fig. 3. *P_Sequence* age-depth for vertical cores drilled at the Lucky Lady site. Models were developed using OxCal version 4.4 (Bronk Ramsey, 2009b) and the IntCal20 calibration curve (Reimer et al., 2020). Calibrated age range uncertainties are shown at 2σ uncertainty.

units to increase fossil recovery. Bulk samples were taken in thin lenses (less than ~10 cm thick) following stratigraphic boundaries. The volume of each sample was about 10–30 kg for organic-rich sediments and 50–100 kg for organic-poor silt. Wet screening of sediment in the field followed Sher and Kuzmina (2007). Briefly here, we used screening boxes (~60 × 40 × 10 cm) with 0.4 mm stainless steel mesh and wet-screened bulk sediment samples to leave an organic-rich residue. Screened and dried sediment was separated into fractions by size, and in the laboratory insect fossils were picked from the fraction >2 mm under light microscopy. The <2 mm fraction was picked under magnification using a binocular microscope. Fossils were identified with reference to collections of modern and fossil insects at the University of Alberta, the Canadian National Collection (CNC) of Insects, Arachnids and Nematodes, and the Moscow Paleontological Museum.

Environmental reconstructions from the insect assemblages were made following the ecological grouping approach presented in Sher and Kuzmina (2007) and Kuzmina (2017). We assigned insect assemblages to nine ecological groups based on the relative proportions of taxa and known habitats, including: s-t – indicators of steppe-tundra environment; dt – dry tundra; mt – mesic and wet tundra; pl – plant litter; sh – shrubs; me – meadow; fo – forest; a&r – aquatic and riparian; and oth – others. We used compound units to indicate fossils that include a secondary environmental group, for example dt(fo), representing taxa living inside the forest zone, but occupying dry open ground. The taxa that make up each of these ecological groups are detailed in Supplementary Materials, Table S3. All fossils were quantified using the Minimal Number of Individuals (MNI) (Elias, 1994). Since MNI reduces over counting of a single individual by assuming that any individual fossil may be represented by its parts, i.e. one head, one pronotum, two elytra, abdomen segments and legs, the MNI is smaller than the number of excavated fossils. In some cases, when the fossils indicate that they belong to different individuals on the basis of differing size or colour, we correct the calculated MNI. This is important for Holocene insect faunas which are characterised by high species diversity and low number of individual species fossils (Kuzmina and Sher, 2006).

2.8. Pore-ice isotopes

We measured pore-ice $\delta^2H/\delta^{18}O$ values from samples taken throughout the Lucky Lady sequence at the University of Alberta using either a LGR (model DLT-100) or a Picarro (model L2130-i) water isotope analyzer, both of which use laser absorption spectrometry. Raw $\delta^2H/\delta^{18}O$ values were normalised to the VSMOW-SLAP scale using water reference materials USGS-45 ($\delta D = -10.3‰$, $\delta^{18}O = -2.24‰$) and USGS-46 ($\delta D = -235.8‰$, $\delta^{18}O = -29.80‰$). Analytical precision in this study was 1.0‰ for δ^2H and 0.2‰ for $\delta^{18}O$ based on routine measurement of an internal secondary water standard. Full results are reported in Supplementary Material, Table S4.

3. Results

3.1. Site stratigraphy, cryostratigraphy and chronology

Chronological data indicates that losseal sediments began to accumulate at Lucky Lady from ca. 17,400 cal yr BP, during the Late Wisconsian (broadly coeval with Marine Isotope Stage; MIS2). Three radiocarbon dated arctic ground squirrel nests from below the prominent paleosol in Unit 1 and range from ca. 16,500 to ca. 13,675 cal yr BP (Table 1). The presence of arctic ground squirrel nests in the lower silts indicate that loess accumulation was initially associated with steppe-tundra vegetation and deep active layers (0.9–1.0 m) (Buck and Barnes, 1999; Zazula et al., 2005). The prominent paleosol (an A horizon), present across the study site contained more than 7% organic carbon (Fig. 5; Table S1), which is at the upper end of the range observed in full glacial paleosols elsewhere in the Klondike goldfields (Sanborn et al., 2006). The irregular boundary of this horizon suggests disruption by cryoturbation, and the 18–30 cm thick C horizon immediately beneath was interpreted as a paleo-active layer because of lower ice content than in the underlying sediment. This indicates that the formation of the paleosol was associated with a substantial shallowing of the active layer. Results from Bayesian *Sequence* model I show the prominent paleosol present near the top of Unit 1 began to develop ca. 13,480 (13,660–13,350) cal yr BP and marks a slowing of loess aggradation. Paleosol development persisted for ca. 220 years, ending ca. 13,260 (13,370–13,180) cal yr BP (Fig. 2). Following the end of paleosol development, accumulation rates increased sharply and remained high until ca. 12,800 cal yr BP (Figs. 2 and 3). These results are consistent with the *P_Sequence* age-depth model

Fig. 4. Photographs of megafauna fossils retrieved from Lucky Lady.

Fig. 5. Photographs of the 2009 Lucky Lady exposure and position of fossil insect samples (indicated by white dots and DL sample numbers). (a) The laterally extensive paleosol and grassy-shrub transition zone (Unit 1/Unit 2) from the left side of the gully shown in Fig. 1c. Other samples from the transition zone were taken from the right side of the gully. (b) Upper part of the Lucky Lady section on the left side of the gully, including a thick organic bed interrupted by silty-sand layer. (c) To right from the gully, the Pleistocene silt (sample DL-B10).

derived from the vertical cores which places the formation of the prominent paleosol ca. 13,470 (13,650–13,340) cal yr BP. Numerous buried A horizons with lower organic content that the preceding paleosol are present throughout this section. These horizons were usually too thin to sample and describe separately, and are consistent with a rapid sedimentation rate, with little opportunity for surfaces to persist long enough to accumulate organic matter before burial. The isotopic ratios in Unit 1 become more enriched with height with pore-ice isotopes ratios from −29.1‰ to −21.2‰ $\delta^{18}O$ and −220.3‰ to −167.7‰ $\delta^{2}H$.

The transition between Unit 1 and Unit 2, is marked by the appearance of *in situ* shrub macrofossils, at ca. 13,210 (13,290–13,140) cal yr BP, only ca. 40 years following paleosol formation. The transition represents a substantial change in sedimentation which becomes dominated by organic accumulation, including abundant woody vegetation. Towards the top of the sequence, a much thicker (20–40 cm) A horizon contained 7.3% organic carbon, although this was from a composite sample, and there were inclusions of mesic (moderately decomposed) peaty material. The latter suggest that organic matter accumulation was occurring under a wet soil moisture regime, while the overall thickness of this horizon indicated a hiatus or slowdown in sediment accumulation. Two radiocarbon dates from the peat and organic rich soils capping the sequence date to the Late Holocene and indicate that these sediments formed much later than the sandy silt and loess deposits below (Table 1). Water isotopes from Unit 2 average between −21.3 and −19.6‰ $\delta^{18}O$ and −168 and −157‰ $\delta^{2}H$. The most enriched values are present near the lower part of the unit.

The chronology shows that there are no substantial hiatuses in deposition between ca. 17,400 and 8000 cal yr BP, other than the slowing of sedimentation associated with development of the paleosol ca. 13,480 cal yr BP (Figs. 2 and 3). This indicates that the Lucky Lady site is the most complete site known from the Klondike across the Pleistocene-Holocene transition.

3.2. Pollen

The lowest two pollen samples with countable palynomorphs are different from all those above. The very high percentages of *Artemisia* (sage) (30–65%) and Chenopodiaceae type (goosefoot or amaranth family) (25–48%), and near absence of tree or shrub pollen, indicate open and probably dry conditions, with very few woody taxa. The goosefoot family is known to be found around saline soils or salty shorelines of ponds or lakes, which are also common in dry environments. Fig. 6 clearly shows this herb-dominated early vegetation cover, with only a few scattered *Betula* (birch) and *Salix* (willow) shrub grains, and no tree pollen.

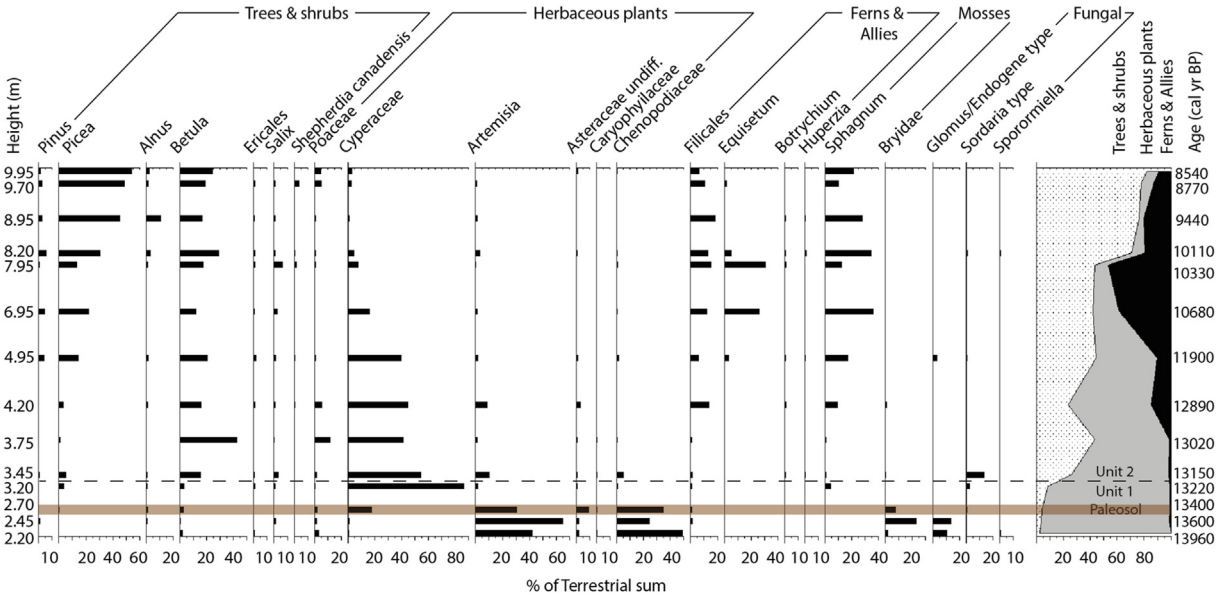

Fig. 6. Pollen analyses from Lucky Lady.

Also notable in the two samples below the paleosol is the presence of various small moss spores (Bryidae) (up to 20%) without any *Sphagnum* (peat moss) spores. Bryophytes are common constituents of exposed soil surfaces in open tundra settings. In addition, the presence of fungal zygospores of the *Glomus* or *Endogene* type suggest some degree of soil erosion during this early phase, since these mycorrhizal soil fungi are associated with the roots of plants, and are only likely to be recovered because of erosion and redeposition in sediments. These indicators of soil instability also suggest an open and erodible surface at the Lucky Lady site prior to development of the paleosol ca. 13,480 cal BP. An interpretation of dry-tundra is supported by the pollen and spores for the pre-paleosol interval, although the low values of Poaceae (grasses) (<5%), are not immediately consistent with reconstructions of steppe-tundra vegetation from elsewhere in eastern Beringia (e.g. Schweger, 1982; Bigelow and Edwards, 2001; Ager, 2003).

Immediately prior to the transition between Unit 1 and Unit 2 Cyperaceae (sedge family) becomes dominant in the pollen assemblage (initially at 90%), replacing herb taxa (*Artemisia* and Chenopodiaceae). Associated with the high sedge abundance are the first appearance of *Sphagnum* and *Picea* (spruce) (4%) pollen, although *Picea* could initially be regional rather than local in origin since *Picea* pollen is well dispersed by wind (local presence is typically inferred from frequencies >10%). At the Unit 1 and Unit 2 transition pollen from shrubs increases rapidly, including *Betula* (likely *Betula nana* or *Betula glandulosa*) pollen which rises from ~2% to ~15%. Together, the pollen assemblage suggests that local conditions became progressively wetter as dry tundra vegetation was replaced by Cyperaceae communities and then shrub tundra from ca. 13,220 cal yr BP.

By ca. 10,680 cal yr BP Filicales (true ferns) and *Equisetum* (horsetail) spores become prominent, along with high values of *Sphagnum* spores (20–35%) and consistently high *Betula* pollen. These changes suggest, along with increasing spruce pollen, that wetter conditions predominated locally, and tree cover increased regionally during this time-period.

3.3. Insect faunas

The Lucky Lady site has excellent permafrost preservation of insect faunas, and 14 bulk samples were collected from the exposure (Table S3). Two of these samples are from Unit 1, including Sample DL-B10 that was collected from 2 m below the prominent paleosol, and sample B9 which was recovered from the paleosol material directly. The next group of samples (DL-B15, DL-B22, DL-B25, DL-B21, DL-B43, DL-B44, DL-B45) were taken from an area of woody macrofossils immediately above the Unit 1/Unit 2 transition. The remaining samples were collected from organic-rich horizons in Unit 2 (Fig. 2).

The lowest sample in the section (DL-B10) dates to ca. 16,500 cal yr BP and was collected from the organic-poor grey sandy silts. The fossil insect assemblage is dominated by steppe taxa (96% of identified taxa). The most abundant member of this group is *Connatichela artemisiae* which represents 88% of the identified individuals. *C. artemisiae* is the only species of the genus *Connatichela,* and is a Beringian endemic weevil whose larvae live in the soil of the Prairie sagewort *Artemisia frigida*, where they feed on its roots (Anderson, 1997). The modern distribution of *C. artemisiae* extends as far north as the Porcupine River, near Old Crow, and south to the Kluane area of southern Yukon where it is associated with disjunct azonal steppe communities (Anderson, 1984, 1997). These communities are found on dry south-facing slopes that are characterised by well drained soils, sagebrush and grasses. The remaining taxa in sample DL-B10 include dry tundra indicators such as *Lepidophorus lineaticollis* (Fig. 7, n = 36) and *Lepidophorus thulius* – both associated with steppe-tundra vegetation (Matthews, 1983). Other taxa include individual fossils associated with mesic tundra (the rove beetle *Aleochara verna*), plant litter (the rove beetle *Quedius* spp.) and riparian environments (the variegated mud-loving beetle *Lapsus tristis)*. The most unusual taxon present is *Lapsus tristis*. These beetles tend to be found close to water and are often found burrowing in wet sand and mud (Crowson, 1981). This is an uncommon association with *C. artemisiae,* but may reflect a small ponding of water in the loessal landscape. Species diversity of the assemblage is low (6 species per 100 MNI).

Sample DL-B9 comes from the prominent paleosol, that can be traced laterally across the exposure, and includes a higher fossil insect diversity than the preceding sample, DL-B10. The assemblage is dominated by the weevil *L. lineaticollis* which represents 74% of

Fig. 7. Photographs of the fossil insects from Lucky Lady. 1 - *Carabus chamissonis* left elytron, D-L-B25; 2 - *Loricera pilicornis*, left el., D-L-B23; 3,4 - *Blethisa catenaria*: 3 – pronotum, D-L-B25, 4 – left el., D-L-B44; 5 *Elaphrus angusticollis*, right el., D-L-B21; 6 – *E. clairvillei*, right el., D-L-B20; 7,8,9 – *E. lapponicus*: 7,8 head, pr., D-L-B22, 9 - right el., D-L-B20; 10 - *Dyschirius hiemalis*, left and right connected el., D-L-B21; 11 *Bembidion arcticum*, right el., D-L-B21; 12 - *Pterostichus arcticola*, pr., D-L-B43; 13 - *Agonum cupripenne*, right el., D-L-B9; 14 - *A. consimile*, right el, D-L-B44; 15 - *Cymindis vaparariorum*, pr, D-L-B24; 16 - *Agabus thomsoni*, left el, D-L-B21; 17 - *Hydroporus tristis*, right el., D-L-B20; 18 - *Agathidium angulare*, pr., D-L-B9; 19 - *Eucnecosum tenue*, left el., D-L-B43; 20,21 - *Olophrum latum*: 20 – pr., D-L-B44, 21 – left and right connected el., D-L-B45; 22 - *Gymnusa atra*, left el., D-L-B20; 23 - *Lathrobium punctulatum*, h., D-L-B23; 24 - *Cercyon cinctus*, left el., D-L-B20; 25,26 - *Megasternum posticatum*, connected h. And pr., right el., D-L-B20; 27 - *Psiloscelis subopaca*, left el., D-L-B20; 28 – Scarabaeidae, leg, D-L-B20; 29 - *Aphodius consentaneus*, left el., D-L-B10; 30 – Byrrhidae, leg, D-L-B22; 31 - *Simplocaria semistriata*, right el., D-L-B45; 32 – *Eanus decoratus*, left el., D-L-B24; 33 - *Chrysomela blaisdelli*, left el., D-L-B25; 34 – *Altica ambiens*, left el., D-L-B23; 35 - *Chaetocnema protensa*, right el., D-L-B24; 36 - *Phyllotreta zimmermanni*, right el., D-L-B20; 37 - *Lepidophorus lineaticollis*, head and pronotum, D-L-B9; 38 *Connatichela artemisiae*, connected left and right el., D-L-B10; 39 - *Pissodes rotundatus*, left el., D-L-B24; 40 - *Rhynchaenus testaceus*, left el., D-L-B23; 41 - *Cossonus crenatus*, right el., D-L-B24; 42 - *Notaris aethiops*, left el., D-L-B24; 43 - *Magdalis gentilis*, right el., D-L-B24; 44 - *Formica podzolica*, h., D-L-B24; 45 - *Camponotus herculeanus*, mandibula, D-L-B24; 46 - *Leptothorax acervorum*, h., D-L-B20; 47 - *Myrmica lobifrons*, h., D-L-B20.

the individuals identified. The remaining taxa include other dry tundra species such as *L. thulius*, the ground beetles *Amara alpina*, *Dicheirotrichus mannerheimi*, the pill beetle *Curimopsis albonotata*, the steppe indicators, including *C. artemisiae* and *Morychus aff. Aeneolus* and the mesic tundra species *Pterostichus arcticola* (Fig. 7, n = 12) and *Pterostichus ventricosus*, as well as single occurrences of riparian and plant litter species. More than 90% of the assemblage is composed of the xerophilous groups (Fig. 10). Forest indicator

species are not present in the assemblage. The species diversity is low (7 species per 100 MNI). The weevil L. *lineaticollis*, which dominates the sample, was one of the most widespread species present in eastern Beringia during the late Pleistocene (Matthews and Telka, 1997). The larvae of *L. lineaticollis* inhabit soils, and modern environmental preference of this species varies from dry and wet tundra to cold steppes, although the beetle is more common in open dry habitats. Observations in the Kluane Lake area show that *L. linaeticollis* is most abundant at the transition from steppe to alpine tundra at the elevation 1400 m (Berman et al., 2011).

The insect assemblages from seven samples spanning the lowest metre of Unit 2 are dominated by mesic tundra (*Pterostichus brevicornis, Pterostichus pinguedineus*), plant litter (*Tachyporus canadensis, Quedius fellmani*), aquatic and riparian indicators (*Olophrum latum*, *Stenus* spp.) (Fig. 7, n = 20,21). Xerophilous groups are secondary. Species diversity through these samples is high (17 species per 100 MNI) taxa), particularly amongst the plant litter group. There are numerous rove beetles, specialist taxa that live in decomposing organic matter and under leaves. Several species belonging to the aquatic and riparian group are also present within these seven samples, including the frequent occurrence of the rove beetle *Olophrum latum* (Table S3). *O. latum* is commonly collected from sedge clumps growing in shallow water (Campbell, 1983). The abundance of *Olophrum latum* is consistent with wetter soils and the sedge remains in the layer. Other indicators of wet conditions include numerous remains of fly pupae and heads of leatherjacket (Tipulidae). We cannot identify these fossils to species level; however, most are fly larvae that inhabit moist habitats. Single forest insects are also present in the seven samples, but are unlikely to record the presence of local forest vegetation. These include the ant *Leptothorax acervorum* (Fig. 7, n = 44), that has been recorded from sites in Alaska up to 150 km north of tree line (Nielsen, 1987), and larvae of the click beetle *Denticollis varians*, commonly found in forest soils and plant litter (Gurjeva, 1989).

Sample DL-B20 comes from a thin organic-rich layer around 1 m above the previous samples. This high in the exposure, steppe insects are rare while forest and meadow indicators are more common. The forest group here includes relatively thermophilous species such as the ground beetle *Elaphrus clairvillei* (Fig. 7, n = 6). This beetle lives on sedge-moss marshland across North America, from New Mexico to Central Alaska; its northern limit is close to the tree line (Goulet, 1983). In the fossil record this species is related to relatively warm conditions or found in southern sites. It has been recorded from the Early Holocene sediments at Eagle River (Bell Basin, northern Yukon), Ikpikpuk River (North Slope of Alaska) and in the late Pliocene Lost Chicken site (Matthews and Telka, 1997; Nelson and Carter, 1987). In Ontario, Michigan, Ohio, Indiana and New York, this species is common in fossil assemblages; typically indicating northern boreal forest (Motz and Morgan, 1997). An Interesting occurrence in this assemblage is the fossil clown beetle *Psiloscelis subopaca* (Fig. 7, n = 27), which lives in ant nests. Modern collection localities for this taxon are concentrated in southern British Columbia and Alberta with only a few in the sites further to the North, including northern Manitoba, and southern and central Yukon (Bousquet and Laplante, 2006). Such disjunctive modern distributions suggest that the species was more broadly distributed in the past. The fossil record supports this assertion, and during the Holocene this species was much more common in Northern areas. Ant remains are also presented in the fossil assemblage DL-B20.

Three samples, DL-B16, DL-B23 and DL-B17 were taken from organic-rich layers in the upper part of the exposure. The first sample from this section includes only single fossils of the steppe weevil *C. artemisiae*, while the two upper samples have no steppe insects. Forest indicators are prominent in these samples and species diversity increases. The forest group includes the ground beetle *Elaphrus clairvillei*, the clown beetle *Psiloscelis subopaca* (Fig. 7, n = 27), the click beetle *Denticollis varians*, the weevil *Rhynchaenus testaceus* (Fig. 7, n = 38), the bark beetle *Scolytus piceae*, and ants (*Camponotus herculeanus;* Fig. 7, n = 43, *Formica podzolica;* Fig. 7, n = 42, *Myrmica* spp. Fig. 7, n = 45). Some of these species are tree related, including *Rhynchaenus testaceus*, that feeds on birch and alder in the boreal forest (Anderson, 1997); *Scolytus piceae* commonly feeds on spruce and only rarely on fir or larch (Bright, 1976).

The youngest sample (DL-B24) was taken from the uppermost peat. This peat is separated from the main section by an unconformity and is Late Holocene in age. The fossil insect assemblage is similar to the two previous samples from the Early-Mid Holocene and includes plant litter, forest, meadow, aquatic and riparian communities along with mesic tundra insects, representing more than 80% of the assemblage. The forest group is rich and includes the click beetles *Denticollis varians, Eanus decorates* (Fig. 7, n = 31), the weevils *Magdalis gentilis* (Fig. 7, n = 41), *Pissodes rotundatus* (Fig. 7, n = 47), bark beetles *Scolytus piceae, Dryocoetes affaber, Ips borealis*, and the ants *Camponotus herculeanus, Formica podzolica and Myrmica* spp. The weevils and bark beetles found in this sample typically feed on spruce conifers.

3.4. Pore-ice isotopes

Co-isotope variability (δ^2H-δ^{18}O) observed in the Lucky Lady pore-ice record is consistent with the interpretation of a meteoric origin. Local precipitation co-isotope variability is characterised by modern δ^2H and δ^{18}O observations from two GNIP (Global Network of Isotopes in Precipitation) stations at Mayo (1986–1989), in central Yukon, and Whitehorse (1961–1965 and 1985–1989), in southern Yukon (IAEA/WMO, 2020). The precipitation data from these sites are defined by a Local Meteoric Water Line (LMWL) with a δ^2H-δ^{18}O slope of 6.5 and an intercept of −28.9‰ (r^2 = 0.98; Fig. 8). Comparatively, the Lucky Lady pore ice measurements fall tightly along the LMWL. A regression line defined by the Lucky Lady pore ice measurements (slope = 6.5 and intercept of −26.7‰) is virtually indistinguishable from the LMWL (Fig. 8), which is strong evidence that the pore-ice are of a meteoric origin. The Lucky Lady pore-ice δ^{18}O record shows an ~8‰ increase across the late Pleistocene, followed by comparatively little variability (~2‰ total range) during the Early-Mid Holocene. The major ~8‰ shift in δ^{18}O occurs at the transition between Unit 1 and Unit 2 and coincides with the expansion of mesic ecological indicators (pollen and plant macrofossils from shrub vegetation, and insect assemblages), suggesting a possible hydroclimatic driver.

4. Discussion

4.1. Interpreting the pore-ice isotopic record

Pore-ice is primarily derived from meteoric waters, the seasonality of which can be strongly influenced by the sedimentological, topographic and hydraulic properties of the site (Porter and Opel, 2020). For example, a pore-ice record from a sloped, peat plateau in central Yukon is defined by strong summer seasonality. This results from rapid, surface and near-surface (upper active layer) drainage of cold-season precipitation during the early melt season and relatively slow drainage of warm-season precipitation, which is favoured to reach the lowermost active layer where hydraulic conductivity is typically 1-2 orders of magnitude lower compared with the upper active layer (Porter et al., 2019). Summer precipitation is also more likely to reach maximum thaw depths in mineral soils such as those found at the Lucky Lady site. In these

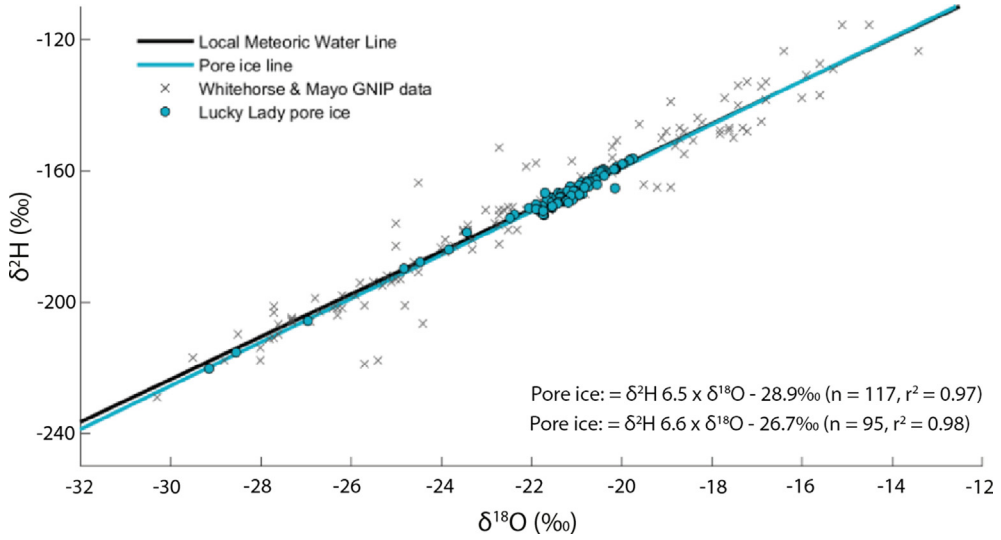

Fig. 8. δ^2H and $\delta^{18}O$ measurements from two local Yukon GNIP stations, Mayo and Whitehorse, plotted on the Local Meteoric Water Line (LMW) (shown as grey crosses). Relict pore-ice δ^2H and $\delta^{18}O$ measurements from the Lucky Lady site, shown as blue circles. The regression line defined by these measurements is shown in blue. (For interpretation of the references to colour in this figure legend, the reader is referred to the Web version of this article.)

settings, however, there is potential for contribution of cold-season precipitation in the deep active layer because of freeze-thaw processes that are unique to fine-grained sediments. For example, in fine-grained sediments underlain by permafrost, the ice content in the upper and lower active layer tends to increase through the winter due to upward and downward migration of residual pore water towards the upper and lower freezing fronts, leaving the middle active layer partially desiccated (Mackay, 1983). Also, during the frozen season, fine-grained sediments develop micro-cracks that serve as conduits for spring meltwater to reach intermediate and lower depths of the active layer, bypassing the physical hydrological constraints imposed by the shallow frost table in spring (Mackay, 1983). Therefore, although the Lucky Lady pore-ice record is principally driven by spring-summer seasonality it is likely to also integrate some cold-season precipitation.

Identifying and quantifying the primary climate control in the Lucky Lady isotopic record is also difficult. The modern isotopic composition of precipitation in central Yukon is strongly influenced by mean air temperature (Porter et al., 2019). However, other factors such as shifting precipitation seasonality and atmospheric circulation (e.g. strength of the Aleutian Low) are likely to have varied across the Pleistocene-Holocene transition and may have imparted some non-temperature-related variability on the Lucky Lady pore-ice record (Fisher et al., 2004; Lasher et al., 2021; Porter et al., 2014, 2016, 2019). Considering the modern precipitation $\delta^{18}O$-temperature sensitivity in this area (0.25‰·°C^{-1}; Porter et al., 2019), in a simple climate interpretation that attributes all pore-ice δ18O variability to change in mean air temperature an ~8‰ increase in $\delta^{18}O$ could be equated to a ~32 °C rise in air temperature, which is unrealistic. Instead, some of the $\delta^{18}O$ change in the Lucky Lady record, and other pre-Holocene Klondike deposits (e.g., Porter et al., 2016), is likely to reflect several hydroclimate changes. Here, we take a conservative approach and simply interpret the Lucky Lady pore-ice isotopic record as a proxy for spring-summer precipitation isotope composition and relate this record to several possible drivers of atmospheric change.

To assess the timing of these isotopic changes, a pore-ice-specific age-depth model is required. Syngenetic pore-ice represents meteoric waters that infiltrated the active layer to the maximum thaw depth, froze *in situ* during the freeze back season and were preserved by the aggrading permafrost table. A process paced by the accumulation of organic and clastic materials at the surface. As such, the depositional age of the pore-ice is always younger than the host sediments. To establish the age of pore-ice, some understanding of the paleo-active layer thickness and sedimentation rate are required (Porter and Opel, 2020). It is likely that during the last cold stage active layers were deeper than at present because sparse vegetation and reduced cloud cover promoted exposed, well drained mineral soils (Guthrie, 1990b, 2001). In this study, we assume cold stage active layers to be 0.8 m (samples from Unit 1 beneath the prominent paleosol), which may be a conservative estimate. This value is between estimates based on the 0.5 m translocation of visible A-horizon material in MIS 4 (Marine Isotope Stage 4) turbic cryosols from the Klondike (Sanborn et al., 2006) and estimates of 1.0 m based on the presence of arctic ground squirrel nests, and their association with active layers at 0.9–1.0 m in modern settings (Buck and Barnes, 1999; Zazula et al., 2005). Other evidence for cold stage active layer depths comes from ice rich layers at ~0.45 m depth beneath the full glacial Kitluk soil - an inceptisol in the Seward Peninsula that likely formed in aggrading loess (Höfle et al., 2000). Active layer depths for the remainder of the record are assumed to be 0.6 m, a median value from modern active layer probing in thickly forested areas (0.5 m) and scattered tree areas (0.6 m) at Dominion Creek (10 km north of the Lucky Lady site) (Fig. 1) (Calmels and Froese, 2009; Calmels et al., 2012). A sharp increase in ice content 18–30 cm beneath the prominent paleosol in the Lucky Lady exposure is interpreted as evidence for a paleo-active layer (see section 3.1) and suggests that at times the active layer may have been even shallower than present.

To test how our assumptions affect the modelled pore-ice ages we applied differing paleo-active layer thicknesses to our chronology (Fig. 9). For cold stage samples, beneath the prominent paleosol, we applied paleo-active layers of 1.0 m (arctic ground squirrel estimates) and 0.45 m (Kitluk soil estimates). For warm stage samples, above the prominent paleosol, we applied paleo-active layers of 0.6 m (active layer at Dominion Creek) and 0.3 m (Lucky Lady paleosol estimate). The results from this experiment show that the choice of paleo-active layer depth affects the age of cold stage samples to a greater extent than warm stage samples. This uncertainty reflects the greater variability in estimates of full

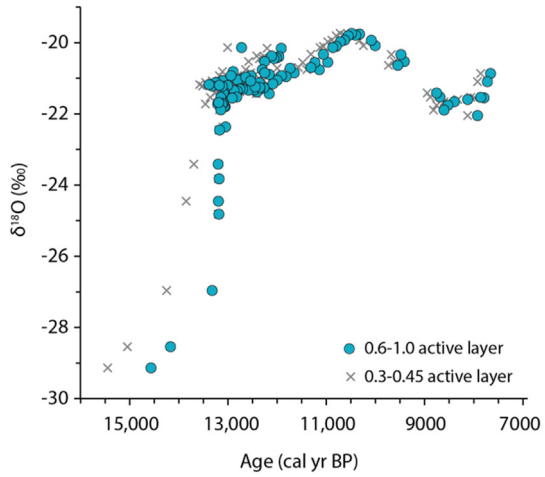

Fig. 9. Pore-ice $\delta^{18}O$ measurements from the Lucky Lady site plotted using alternative palaeo-active layer depths (median age cal yr BP). Cold stage samples (below the prominent paleosol) are plotted with 0.45–1.0 m active layer depths. Warm stage samples (above the prominent paleosol) are plotted with 0.3–0.6 m active layer depths.

glacial palaeo-active layer depths and the slower rate of accumulation at Lucky Lady during this time-period. Variability between warm stage samples with different chosen paleo-active layer depths is substantially reduced by the rapid accumulation of loessal sediments, and in places the median age difference between paleo-active layer depths of 0.3 and 0.6 m is as little as 15 years. Importantly, the choice of paleo-active layer depth does not alter the timing of isotopic shifts relative to vegetation changes at Lucky Lady.

4.2. Full glacial environments

4.2.1. What was the local vegetation composition at the Lucky Lady site?

The oldest samples from the Lucky Lady site date to the Late Wisconsinan (broadly coeval with MIS2) and represent near full glacial conditions. The fossil insect fauna, pollen assemblages and the presence of arctic ground squirrel nests all indicate an arid landscape, with deep active layers, that supported elements of steppe-tundra vegetation. The abundance of *C. artemisiae* remains (88% of the identified individuals) and pollen frequency from *Artemisia* (65-42%) and Chenopodiaceae (49-25%) suggests that herbaceous taxa formed an important part of the local vegetation. Conversely, Poaceae pollen is infrequent (3-2%) and shrubs are almost absent (*Betula* 2-1%, *Salix* 1-0%). These relative vegetation assemblages appear to differ from steppe-tundra reconstructions in other areas of eastern Beringia, although exact comparison is complicated by chronological ambiguity. For example, in western Alaska, *Artemisia* macrofossils are near-absent ("one doubtfully identified seed") from the buried, full glacial, Kitluk paleosol on the Seward Peninsula (Goetcheus and Birks, 2001), while Poaceae pollen is dominant in Late Wisconsinan samples from Zagoskin Lake (45–65%) (Ager, 2003). In pollen records from interior Alaska, Poaceae is also prominent in steppe-tundra samples - reaching 54% at Windmill Lake (Bigelow and Edwards, 2001) and ~30% at Lost Lake (Tinner et al., 2006). A west-east precipitation gradient was hypothesised by Guthrie (2001) and the presence of *C. artemisiae* remains, which is not found outside of easternmost Beringia during the Pleistocene, coupled with abundant *Artemisia* and Chenopodiaceae pollen relative to other areas of eastern Beringia, may indicate regional hyper-aridity, caused by the presence of the Cordilleran–Laurentide ice sheet complex (Zazula et al., 2006).

4.2.2. Evidence for warm soil temperatures in full glacial environments

The insect assemblages at the Lucky Lady site indicate that Late Wisconsinan soil temperatures may have been mild in spite of reduced air temperatures. *C. artemisiae* is a relatively thermophilous species and does not entirely follow its host plant north where *Artemisia frigida* reaches the Arctic coast (Cody, 2000). The coldest modern distribution of *C. artemisiae* is Kluane Lake, southwest Yukon (Berman et al., 2001), where the average July air temperature is 13.1 °C (Burwash monitoring station, Environment Canada Climate Normals, 1981–2010). The warm soil temperatures and abundance of exposed mineral soil in the areas of *Artemisia frigida* are likely to be important since weevils with ground larvae are usually sensitive to soil temperature. In Asia, a functionally similar lifestyle is associated with another weevil; *Stephanocleonus eruditus*, whose larvae live on plant roots in the steppe communities. These weevils are also known to be thermophilous and their modern distribution suggests that mean July air temperatures were at least 10–11 °C in west Beringia during periods of MIS2 (Alfimov and Berman, 2001, Alfimov and Berman, 2001). These warm soil indicators contrast other proxy records that suggest air temperatures were substantially reduced in Beringia during MIS2 (e.g. Kurek et al., 2009a, 2009b), including the $\delta^{18}O$ record from the Lucky Lady site. Although it is difficult to accurately quantify late Pleistocene air temperatures based on the $\delta^{18}O$ record, the strongly depleted pore-ice $\delta^{18}O$ measurements suggest some local cooling during the late Pleistocene. The apparently conflicting information regarding local summer temperatures from insect fossils and the pore ice $\delta^{18}O$ record can be reconciled by Guthrie's (2001) explanation of the productivity paradox and the differing relations between air temperatures and soil temperatures during the Pleistocene cold stages and the Holocene. During the late Pleistocene, the arid and inorganic soils (evident from palaeoecological analyses at Lucky Lady) would have responded rapidly to spring/summer air temperatures as cloudless skies, limited snow cover and absence of leafy, surface organic matter meant soil temperatures quickly rose in spring. As a result, lower summer air temperatures may still have promoted warm soil temperatures. In contrast, Holocene soils would have been (and still are) insulated from warmer spring air temperatures by more frequent cloud cover, deeper winter snow and organic-rich, peaty soils.

4.3. Late glacial environments and shrub expansion

4.3.1. How did the environment change at the Lucky Lady site?

At Lucky Lady, the collapse of the mammoth steppe ecosystem (and disappearance of steppe-tundra vegetation) began with a slowing of loess accumulation and development of the prominent paleosol at ca. 13,480 cal yr BP. The 18–30 cm thick paleo-active layer, immediately beneath the palesol (indicated by lower ice content and C horizon) suggests that active layers became substantially shallower at this time. Steppe-tundra vegetation indicators including; *Artemisia* pollen and *C. artemisiae* (steppe weevil) remains, decline and are replaced by *Cyperaceae* and xerophilous insect groups linked with dry tundra. Environmental DNA analyses suggest that the formation of the paleosol is associated with the appearance of woody vegetation including increasing *Salix*, *Alnus*, *Betula*, *Populus* and *Ericaceae*, as well as ground nesting birds such as *Lagopus* (willow ptarmigan) that rely on shrub vegetation (Fig. 10) (Murchie et al., 2021b). Pollen and plant macrofossil remains from shrub taxa; however, are largely absent (2% *Betula* pollen, 0% *Salix* pollen) until the transition from Unit 1 to Unit 2 (80 cm above the paleosol) ca. 13,210 cal yr BP. Together, the

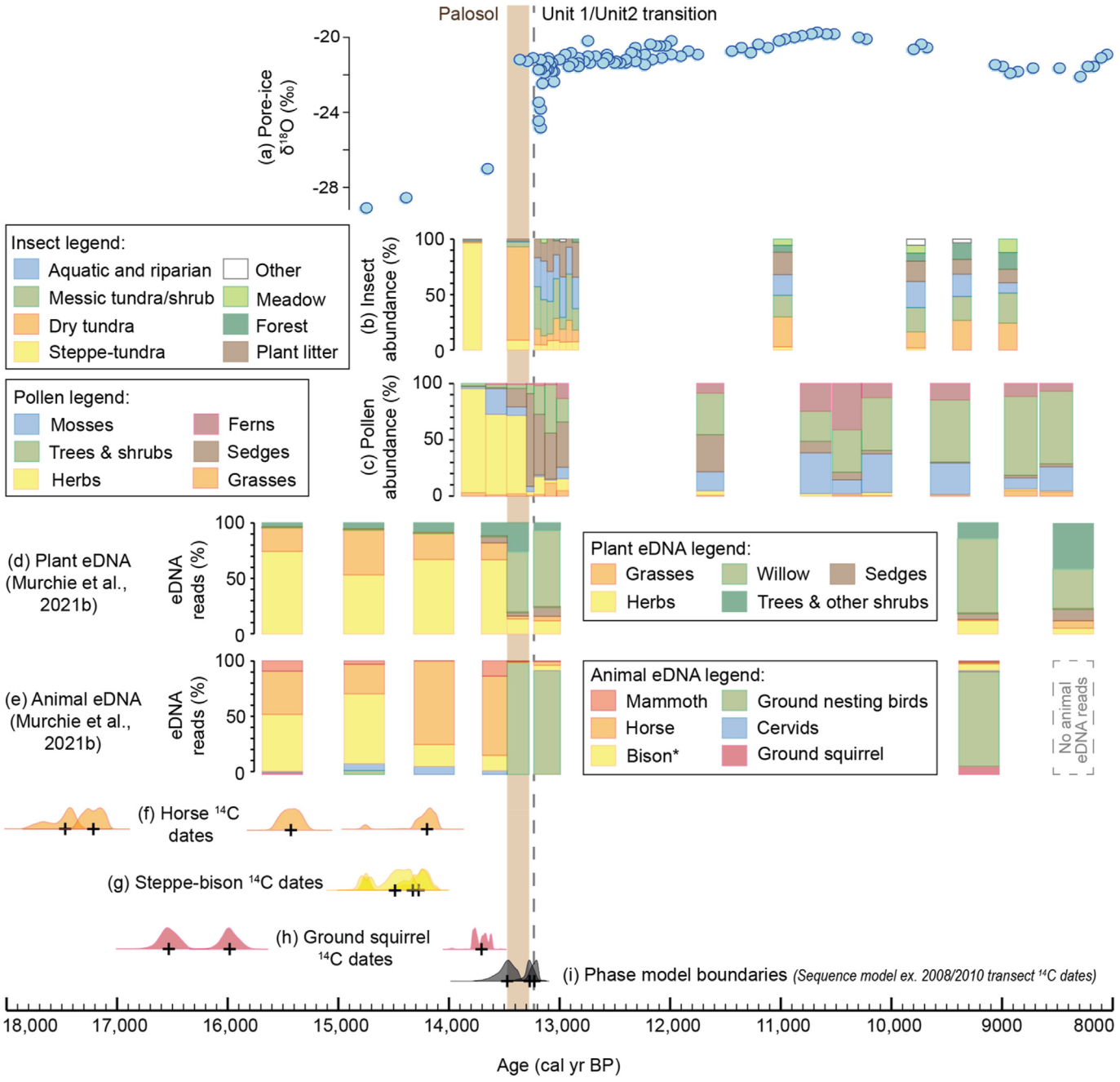

Fig. 10. Palaeoenvironmental data from the Lucky Lady site (a) Pore-ice $\delta^{18}O$ measurements. (b) Fossil insect ecological groups (c) Pollen summary groups. (d) Plant eDNA summary – normalised number of reads (Murchie et al., 2021a, 2021b). (e) Animal eDNA summary – normalised number of reads (Murchie et al., 2021a, 2021b). *Note that bison reads includes a minor contribution from Dall's sheep. (f–h) Calibrated radiocarbon dates from megafauna fossils and arctic ground squirrel middens. (i) Modelled Oxcal probability density functions for the prominent paleosol and Unit1/Unit 2 transition.

ecological evidence indicates that the establishment of the paleosol was associated with increasing moisture availability at Lucky Lady. The xerophilous insect assemblage and absence of abundant shrub pollen and macrofossils suggest that this increase was subtle and may have been restricted to poorly drained areas of the valley floor where conditions were wetter. A similar pattern is observed in some high-resolution pollen records from lake-sediments in eastern Beringia, where declining *Artemisia* and increasing *Cyperaceae* pollen predate the birch rise, and are attributed to slight increases in moisture (e.g. Windmill Lake, Bigelow and Edwards, 2001).

Following the culmination of paleosol development, ca. 13,260 cal yr BP, sedimentation rates increase sharply at Lucky Lady - accumulating 80 cm of material in only ca. 40 years. This may represent a 'sweet spot', that is also evident in loess records from interior Alaska, where despite moderate changes in aeolian activity increasing vegetation cover enhanced loess entrapment and accumulation (Muhs et al., 2003). Pollen analyses from this interval are almost entirely composed of *Cyperaceae* (86%), which is also abundant in the eDNA reconstruction, indicating a continued increase in moisture availability (Murchie et al., 2021b).

The transition between Unit 1 and Unit 2 is marked by the

appearance of woody macrofossils that represent the local development of shrub tundra. Insect assemblages from immediately above this transition are dominated by mesic tundra, plant litter, aquatic and riparian indicators, while *Betula* pollen becomes increasingly abundant. Pore-ice $\delta^{18}O$ isotopes also shift rapidly at this transition indicating that the ecological transitions observed at the Lucky Lady site were associated with substantial hydroclimate changes. Following the establishment of shrub tundra ca. 13,210 cal yr BP environmental changes become more gradual.

4.3.2. How abundant were different shrub taxa and when did they become established at the Lucky Lady site?

Establishing the timing of shrub expansion and relative abundance of *Salix* and *Betula* is important for understanding the role of vegetation change in late Quaternary megafauna extinctions. In eastern Beringia, woolly mammoth and horse were both extirpated as shrub tundra replaced steppe-tundra vegetation at the end of the Pleistocene (Guthrie, 2001, 2006; Mann et al., 2013, 2015). While birch shrubs produce toxic anti herbivory compounds, spring willow shoots/leaves are highly nutritious and exploited by extant megafauna including moose (*Alces*) and reintroduced Alaska wood bison (*Bison athabascae*) (Guthrie, 1984, 2006). Therefore, some shrub taxa may have initially been a benefit to megafauna while others are likely to have been a hindrance. Both Monteath et al. (2021) and Murchie et al. (2021b) hypothesise that because *Salix* is an 'under producer' of pollen relative to *Betula* it is obscured in the pollen sum and may have been more abundant amongst shrub tundra vegetation than recognised in palynology. In many lake-sediment records *Salix* pollen increases prior to *Betula* and the plant macrofossil record from eastern Beringia is dominated by *Salix* remains, supporting this interpretation (Monteath et al., 2021). The multi-proxy palaeoecological data from Lucky Lady provides a means to test this hypothesis; however, determining the relative abundance of *Salix* is not straightforward in this record. *Salix* eDNA reads are frequently an order of magnitude greater than any other taxa suggesting that willow was a dominant component of the local shrub tundra (Murchie et al., 2021b) (Fig. 10). However, *Salix* pollen never represents more than 6% of the pollen sum (rarely exceeding 1%) and willow eDNA is abundant in samples where both *Salix* pollen and shrub macrofossils are absent (Fig. 10). Discrepancies between our proxies could represent either: i) differing spatial signals (local vs regional), ii) vertical re-working, iii) eDNA release, recovery or capture biases or iv) real dominance of *Salix* in late Pleistocene shrub tundra.

i) *Salix* eDNA is abundant in analyses from the prominent paleosol despite an absence of *Salix* pollen or shrub macrofossils (Murchie et al., 2021b) (Fig. 10). It is possible that these inconsistent results are caused by the differing spatial signals captured by our proxies. Pollen data represents a combined signal from vegetation surrounding the study site, whereas, eDNA in frozen sediments is derived from a more local scale, and *in situ* macrofossils directly represent the vegetation at the study site (Arnold et al., 2011; Edwards et al., 2018). It may be that during the formation of the prominent paleosol *Salix* was rare at the Lucky Lady site relative to other plant taxa, as indicated by pollen and plant macrofossil analyses. In this scenario eDNA must have been reworked from wetter areas of the creek valley (where *Salix* was present) by fluvial or aeolian process. This seems unlikely however, as the sedimentology at Lucky Lady is not consistent with fluvial deposition and DNA is rapidly degraded in UV light (Pang and Cheung, 2007), limiting its aeolian transport potential. Some proportion of the *Salix* eDNA signal could be from airborne eDNA (Clare et al., 2021) although this does not explain the dominance of *Salix* in our samples. Further, eDNA from willow ptarmigan (*Lagopus*) is also abundant in the same sample (Fig. 10), which produced a high coverage (43.8X) mitochondrial genome (Murchie et al., 2022). This species of ground-dwelling bird subsists on willow buds (and insects) and nests in shrub thickets of willow and alder, further indicating the presence of local willow. It therefore seems unlikely that such abundant *Salix* and *Lagopus* eDNA would survive off-site erosion and transport to the degree that their signals would exceed all other eDNA in the sample.

ii) Alternatively, the abundance of *Salix* eDNA prior to pollen and macrofossil evidence could be caused by vertical reworking in the active layer. Although reworking is unlikely once sediments become permanently frozen, eDNA in perennially frozen deposits is susceptible to vertical movement due to its exceptional preservation, which in some contexts has been shown to facilitate the survival of low abundance ancient eDNA through erosion, transport, and reincorporation processes (Arnold et al., 2011). The Lucky Lady pore-ice isotopic record demonstrates that the sediments have not thawed since becoming permafrost, but it is possible that eDNA from above the Unit 1/Unit 2 transition (where shrub macrofossils are abundant) was reworked downward prior to this.

iii) The discrepancy between pollen and eDNA evidence from *Salix* and *Betula* abundance may be caused by different means of preservation and identification amongst these proxies in loessal sediments (Pedersen et al., 2013; Parducci et al., 2015). Murchie et al. (2021a, 2021b) targeted the genes *rbc*L, *trn*L, and *mat*K in the chloroplast genome for the taxonomic identification of plants. This plastid is generally maternally inherited in angiosperms as there are organellar degradation pathways that breakdown chloroplast DNA in pollen (Bell et al., 2016). As such, the *Salix* DNA signal detected here likely originated from macro-tissue degradation of litter fall and general biomass turnover, and is not measuring DNA from pollen. *Betula* and *Salix* are equally represented in the Palaeochip Arctic v1.0 bait-set (84 and 85 unique baits respectively), suggesting that the over-representation of *Salix* relative to *Betula* is caused by different eDNA inputs rather than capture bias in the eDNA methods.

iv) Finally, it is possible that *Salix* was a dominant part of the local shrub tundra vegetation as suggested by eDNA results from Lucky Lady and other permafrost exposures in Klondike (Murchie et al., 2021b). If this was case, locally, and elsewhere in Beringia, then unpalatable vegetation (*Betula*) may not have affected megafauna as strongly as previously suggested (Guthrie, 1984, 2001) – although it is important to note that dietary niches of late Pleistocene megafauna are complex and *Salix* may not have sufficiently replaced grazing resources. Therefore, it is important to ask; *was shrub tundra inhospitable to all megafauna* and if so *why*? It may be that some megafauna taxa would have persisted in spite of the vegetation change were it not for the presence of humans who were present in eastern Beringia from at least ca. 15,000 cal yr BP (Potter et al., 2017). Megafauna inhabited eastern Beringia throughout the Middle Wisconsinan interstadial (MIS3) when a similar shrub expansion took place and humans were absent (Guthrie, 2006; Mann et al., 2013). However, it is difficult to interpret how grazing megafauna were impacted by earlier shrub expansions as the population dynamics of late Pleistocene megafauna taxa are unclear (Guthrie, 2006; Mann et al., 2013) and warm stages may have varied substantially (Meltzer, 2020). It is possible that other

environmental changes associated with shrub tundra expansion may have been important controls of megafauna abundance. For example, increasing snow depth, insect harassment, widespread paludification and thermokarst would all have negatively impacted large, grazing mammals (Mann et al., 2015). These uncertainties highlight the need for further multi-proxy palaeoenvironmental study if we are to understand the relative roles of climate and humans in Late Quaternary extinctions.

4.4. Early Holocene environments

At Lucky Lady, Early Holocene environments are characterised by gradual vegetation transitions and increasing forest indicators. Around 11,900 cal yr BP Picea becomes established in the local environment and *Sphagnum* continues to grow in importance. From 10,680 cal yr BP Filicales, *Equisetum*, *Sphagnum, Betula* and Picea are dominant, replacing Cyperaceae in the pollen sum. After ca. 10,680 cal yr BP Picea becomes increasingly important within the pollen sum, rising from 30% to >50%. Insect assemblages also become dominated by forest indicators at this time, including the bark beetle *Scolytus piceae*, and together this evidence is consistent with the establishment of full taiga/boreal forest in central and southern Yukon ca. 10,000 cal yr BP (Bunbury and Gajewski, 2009).

These gradual vegetation transitions are more subtle than those that took place at Lucky Lady during the late Pleistocene and may have been driven by a combination of climate controls and positive feedback loops. For example, increasing in shrub and boreal taxa are suggested to have had a regional warming effect (Bartlein et al., 2015). The climate of the Early Holocene is hypothesised to have been highly variable with strong regional and temporal fluctuations (Kaufman et al., 2016). At Lucky Lady, however, vegetation transitions are unidirectional and are characterised by continual increases in boreal taxa, indicated by pollen, eDNA and insect assemblages. This suggests that in central Yukon either climate reversals were not substantial enough to alter vegetation succession or, site specific controls (e.g. Lucky Lady is north facing), local environmental conditions and positive feedback loops were more important. It may also be the case that some climate controls, such as the progressive flooding of the Bering Land Bridge, were muted in central Yukon because of greater continentality.

The local establishment of Picea at Lucky Lady ca. 11,900 cal yr BP is amongst the earliest reliable indicators for spruce re-establishment in eastern Beringia following the Last Glacial Maximum. Although older Late Wisconsin examples have been reported, many of these are derived from radiocarbon dates on bulk lake-sediment which are now known to be unreliable (e.g. Cwynar, 1982). The early establishment of Picea at Lucky Lady could hint at a Late Wisconsin spruce refugia or represent some of the first colonisers through the ice free corridor which had opened before 13,200 cal yr BP (Heintzman et al., 2016).

4.5. When did the mammoth steppe ecosystem collapse at Lucky Lady?

At Lucky Lady, the robust chronology and rapid rates of accumulation mean that the collapse of the mammoth steppe ecosystem can be defined by several different lines of evidence with varying ages. The first of these is the establishment of the prominent paleosol in Unit 1, ca. 13,480 cal yr BP. Below this, classic indicators of steppe-tundra vegetation are present including arctic ground squirrel nests and abundant indicators of *Artemisia* (*C. artemisiae* remains and pollen). With development of the paleosol, *Artemisia* indicators decline and are replaced by more mesic vegetation (e.g. Cyperaceae), including eDNA evidence for shrub taxa (Murchie et al., 2021b). Although beetle assemblages show that this new environment was still comparatively arid, the absence of prominent steppe-tundra indicators suggests that the substantial vegetation change had begun by this time.

Secondly, the transition between Unit 1 and Unit 2, ca. 13,210 cal yr BP, represents the local establishment of a new wide spread environment - shrub tundra. This transition is observed in pollen records from across eastern Beringia where rapid increases in *Betula* (often to >50% of the pollen sum) indicate wetter conditions and a shallowing of active layers (Anderson et al., 2003). The establishment of shrub tundra marks the transition to a new, environment that was clearly very different from the mammoth steppe. Although elements of the mammoth steppe ecosystem may have persisted (e.g. megafauna) the cold, arid-adapted steppe-tundra vegetation had been largely replaced at Lucky Lady by this time.

Finally, Guthrie (1982) argued that conceptually the late Pleistocene, steppe-tundra vegetation mosaic could be defined by the megafauna that inhabited it. At Lucky Lady, faint eDNA signals hint at late survival of horse and woolly mammoth for sometime after the establishment of boreal forest during the Early Holocene (Murchie et al., 2021a, 2021b). The youngest of these samples dates to ca. 9180 cal yr BP and post-date the final radiocarbon dated remains from these taxa at the site (Table 2), and elsewhere in eastern Beringia (Guthrie, 2006; Mann et al., 2013), by several thousand years. Although steppe-tundra indicators remain present until this time (e.g. low *Artemisia* pollen frequencies and megafauna eDNA) the vegetation community is starkly different from the late Pleistocene and it is difficult to argue that the mammoth steppe ecosystem persisted into the Holocene in central Yukon.

4.6. Late Pleistocene vegetation transitions across eastern Beringia

4.6.1. What drove the collapse of the mammoth steppe?

During the late Pleistocene, climate in eastern Beringia was influenced by increasing summer insolation, rising atmospheric CO_2 concentrations, progressive flooding of the Bering Land Bridge and the collapsing North American ice sheets, all of which may have affected central Yukon differently (Bartlein et al., 1991). We know from the expansion of shrub tundra, increasing lake levels, widespread thermocarst and peatland initiation that the environment became substantially wetter from around 15,000 cal yr BP (Hopkins, 1982; Abbott et al., 2000; Jones and Yu, 2010; Walter et al., 2007). However, the climate controls that drove these changes are less clear. Two principal climate-driven hypotheses have been advanced to explain late Pleistocene vegetation transitions across eastern Beringia.

Firstly, Anderson (1985, 1988) suggested that progressive flooding of the Bering Land Bridge provided an expanding moisture source that enhanced precipitation in western Alaska before more central and eastern areas. In modelling experiments Bartlein et al. (2015) found that under Early Holocene boundary conditions the flooding of the Bering Land Bridge reduced seasonality in eastern Beringia – promoting cooler summers and warmer winters. The precise timing and effects of progressive flooding during the late Pleistocene, however, are less clear. Alternatively, Bartlein et al. (1991) suggested that increasing moisture was caused by changes in the atmospheric circulation and the development of more pronounced westerlies over eastern Beringia. This hypothesis has been reiterated by subsequent modelling studies and linked with lowering of the Cordilleran and Laurentide ice sheet complex, and a northward movement of the westerly jet (Bartlein et al., 2014; Lora et al., 2016).

Testing these hypotheses using available palaeo records is largely dependent on the chronology of shrub tundra expansion,

inferred from *Betula* pollen (Abbott et al., 2010). During the late Pleistocene, dwarf birch taxa existed in sheltered refugia across eastern Beringia where winter snow depth provided sufficient moisture and insulation (Brubaker et al., 2005). As conditions became warmer and wetter these low growing shrubs expanded rapidly across the landscape and as productive pollen producers are well recorded in lake-sediment records. If the hypothesis of Anderson (1985, 1988) is correct shrub tundra would be expected to expand earlier in western Alaska than more central and eastern areas of eastern Beringia. Conversely, if the Bartlein et al. (1991) hypothesis is correct then changes in vegetation should occur synchronously across the region. As the most precisely dated record of shrub tundra expansion in eastern Beringia the Lucky Lady sequence is particularly valuable for addressing these hypotheses.

At present, there is no clear west-east pattern in the timing of *Betula* expansion when considering AMS radiocarbon dated lake-sediment records (Monteath et al., 2021). The only palaeoenvironmental records from the eastern margins of Beringia that meet these chronological criteria and span this time-period are Hanging Lake (Kurek et al., 2009a) and Trout Lake (Irvine et al., 2012), in Northern Yukon. Both of these records place the beginning of shrub tundra, and expansion of *Betula*, ca. 13,800 cal yr BP. In western Alaska, the timing of *Betula* expansion varies between ca. 14,800 cal yr BP at Ruppert Lake (McGowan et al., 2018) and ca. 13,600 cal yr BP at Arolik Lake (Hu et al., 2006). Therefore, there is no consistent evidence for a progressive west-east expansion of shrub taxa that would support the Anderson (1985, 1988) hypothesis. However, the Bartlein et al. (1991) hypothesis is also not well supported by the available palaeoenvironmental data. Replicated pollen records from lake-sediments across eastern Beringia indicate that at some sites shrub tundra expansion began up to a millennium earlier than at Lucky Lady (e.g. Bigelow, 1997; Higuera et al., 2008; Abbott et al., 2010; McGowan et al., 2018). These include Lake of the Pleistocene, on the North Slope, where rapid increases in *Betula* pollen are constrained to ca. 14,400 cal yr BP by replicated AMS radiocarbon dates on shrub macrofossils (Mann et al., 2002).

At present, existing palaeoecological data is not consistent with either hypothesised or modelled projections of climate change during the late Pleistocene. It is likely that this uncertainty is caused by the difficulty in developing chronology from high-latitude lake-sediments that make up the majority of the palaeo records from this region (Abbott and Stafford, 1996). The Lucky Lady sequence clearly demonstrates the potential for developing robust age models from permafrost exposures. Similar work has been undertaken at the Carter Section and drained Lake of the Pleistocene where exposed sediments can be examined for macrofossils suitable for radiocarbon dating (Mann et al., 2002; Gaglioti et al., 2018), and together these sites set a chronological standard that must be replicated if millennial scale climate trends are to be identified and understood. It is interesting to note that the expansion of shrub tundra at Lucky Lady is substantially later than most AMS dated records from eastern Beringia. The majority of these place this transition close to, or shortly after, 14,000 cal yr BP (Monteath et al., 2021). This implies a local climate control had a strong influence on the environment of central Yukon during the late Pleistocene. The most likely cause is the proximity of the Cordilleran–Laurentide ice sheet complex which may have influenced atmospheric dynamics, isotope distillation, source region of the precipitation, and possibly precipitation seasonality. The shift in pore-ice $\delta^{18}O$ measurements and local expansion of shrub tundra (ca. 13,210 cal yr BP) at Lucky Lady falls within a period of rapid glacial retreat (Heintzman et al., 2016; Norris et al., 2022; Stoker et al., 2022), supporting this hypothesis.

4.6.2. Is the Younger Dryas climate reversal evident in Klondike, central yukon?

Interestingly, we do not find any evidence for a Younger Dryas climate reversal in our palaeoenviromental data from Lucky Lady. Although sampling resolution for pollen, eDNA and insect analyses may preclude this, high-resolution $\delta^{2}H$ and $\delta^{18}O$ measurements span this interval. The absence of a Younger Dryas isotopic signal at Lucky Lady may represent either: i) overprinting of the record by deeper Holocene active layers, ii) a limited/absent climate reversal in central Yukon or iii) proxy sensitivity.

i) It is possible that active layers deepened during the Early Holocene as summer temperatures exceeded late Pleistocene values without substantial changes in vegetation cover before the establishment of Boreal forest ca. 10,000 cal yr BP. This could have overprinted the Younger Dryas $\delta^{2}H$ and $\delta^{18}O$ signal with Holocene values and removed any climate reversal from the record. At Lucky Lady, accumulation rates during the Younger Dryas time-period are lower than the preceding period, however, remain above 0.1 cm yr^{-1}, and span more than a metre of sediment (Figs. 2 and 3). Therefore, in order to overprint the entire time-period the active layer would need to have become substantially deeper. Given that the active layer appears to have become shallower at Lucky Lady as shrub tundra became established, and modern active layer depths vary between locally between 60 and 50 cm (Calmels and Froese, 2009; Calmels et al., 2012), this seems unlikely.

ii) Alternatively, the Younger Dryas climate reversal may not have been well expressed in central Yukon. Strong climate variability has been reported from pore-ice and fossil *Salix* $\delta^{18}O$ measurements on the North Slope (Meyer et al., 2010; Gaglioti et al., 2017), as well as pollen and glacial studies in southwest Alaska (Hu et al., 2006; Young et al., 2019), however, in a review of published records spanning the Younger Dryas time-period Kokorowski et al. (2008) found that a climate reversal was largely absent in interior eastern Beringia. High resolution pollen records from central Alaska show only very subtle responses to Younger Dryas cooling and it may be that any climate reversal at this time was comparatively modest in central Yukon (e.g. Bigelow and Edwards, 2001).

iii) Finally, the seasonal/climate sensitivity of the Lucky Lady pore-ice $\delta^{2}H/\delta^{18}O$ record may preclude the preservation of a Younger Dryas climate reversal. Cooling during the Younger Dryas is argued to have been more pronounced during winter (Denton et al., 2005). As the pore-ice $\delta^{2}H/\delta^{18}O$ signal is principally driven by spring/summer hydroclimatic it is possible that the record is insensitive to climate changes associated with the Younger Dryas reversal. Similarly, the Lucky Lady pore-ice $\delta^{2}H/\delta^{18}O$ record is likely to be sensitive to climate controls beyond temperature such as changing atmospheric circulation linked with deglaciation (Porter et al., 2016). If these controls are responsible for the majority of the late Pleistocene shift in $\delta^{18}O$ then cooling associated with the Younger Dryas may not be registered in the record.

4.7. Implications for contemporary high-latitude ecology

The rapid transition from steppe-tundra to shrub tundra at Lucky Lady has parallels with contemporary shrub expansion that is affecting large areas of the Arctic. Today, anthropogenic-driven warming is causing shrubs to expand northwards - particularly along river valleys and other areas of disturbed ground (Sturm et al., 2001; Tape et al., 2006). This rapid vegetation change has

implications for soil temperatures, carbon storage and faunal distributions (Myers-Smith et al., 2011). The Lucky Lady record demonstrates that shrub vegetation responds rapidly to changes in hydroclimate and can become dominant within the landscape in ca. 40 years. The record also reiterates the sensitivity of insect communities to environmental change. At Lucky Lady, assemblage turnover was completed within decades as soil conditions and vegetation changed. Similar changes are likely to occur in response to current shrub expansion with wider implications for food webs across the Arctic.

The expansion of shrub tundra at Lucky Lady coincided with sharp changes in atmospheric conditions, inferred from pore-ice $\delta^{18}O$ measurements (Fig. 10). This indicates that in central Yukon the collapse of the mammoth steppe ecosystem was a bottom up, climate-driven process, and adds to a series of studies that show climate was the primary control of late Pleistocene vegetation rather than top-down pressure from megafauna (Guthrie, 2001, 2006; Mann et al., 2013, 2015; Rabanus-Wallace et al., 2017; Monteath et al., 2021). Together, these studies suggest that large-scale geoengineering proposals, aiming to restore the mammoth steppe through re-wilding, would be unsuccessful (Zimov, 2005).

5. Conclusions

Permafrost-preserved loessal sediments in the Klondike Placer District of central Yukon record the collapse of the mammoth steppe ecosystem in exceptional resolution. Pollen, fossil insect assemblages and the presence of arctic ground squirrel middens indicate that Late Wisconsinan (MIS2) environments were characterised by xeric, steppe-tundra vegetation and deep active layers. The presence of thermophilous insect taxa (*C. artemisiae*) suggests that summer soil temperatures may have been similar to present day. This contrasts with strongly depleted pore-ice $\delta^{18}O$ measurements, which indicate colder spring-summer air temperatures, and is best explained by Guthrie's (2001) productivity paradox model, whereby shallower snow cover, inorganic soils and cloudless skies promoted warmer growing season soil temperatures. The collapse of the mammoth steppe ecosystem began at Lucky Lady ca. 13,480 cal yr BP with the development of paleosol. At this time turnover in insect communities, declining *Artemisia* abundance and the first indication of shrub taxa eDNA (Murchie et al., 2021b) all suggest subtle increases in moisture availability. Shrub tundra became dominant at the site in as little as 40 years, ca. 13,210 cal yr BP. This transition coincides with rapid changes in pore-ice $\delta^{18}O$ measurements and lags other areas of eastern Beringia by up to 1000 years. This delayed expansion of shrub tundra probably reflects the local influence of the Cordilleran–Laurentide ice sheet complex on regional climate. The rapid expansion of shrub tundra at Lucky Lady has parallels with contemporary shrub expansion in high-latitudes and illustrates that insect communities are likely to change rapidly in response to climate change with implications for wider Arctic food webs.

Author contributions

SK, MM, FC, PS, GZ, BS, HP and DF completed fieldwork and collected samples. AJM developed Oxcal age models, helped to interpret data and wrote the manuscript with input from SK and DF. SK analysed and interpreted fossil insect remains. MM analysed pore-ice isotopes. MM and TP interpreted pore-ice isotopes. RM analysed and interpreted pollen assemblages. PS described and interpreted soils data. BS, TJM and HNP analysed and interpreted eDNA. DF conceived and designed the project. All authors contributed to the writing of the manuscript.

Declaration of competing interest

The authors declare that they have no known competing financial interests or personal relationships that could have appeared to influence the work reported in this paper.

Data availability

All data is available either in the manuscript of SI.

Acknowledgements

This research was supported by the Future ArcTic Ecosystems (FATE) research consortium, as well as grants from the Natural Science and Engineering Research Council of Canada (to DF, RM and HNP) and Canada Research Chairs Program (to DF and HNP). Insect research was supported by the Russian Foundation for Basic Research (n. 20-04-00165a). Harvey Friebe assisted with pollen sample preparations. We would like to thank the placer gold mining community in the Klondike and the Tr'ondëk Hwëchin for continued support of our research in their Traditional Territory. We dedicate this article to the memories of John V. Matthews, Jr. and Alice Telka, two pioneering paleoecologists who provided the foundation for studies of environmental change in Beringia, and the use of fossil insects for paleoecological reconstructions. We are grateful to Benjamin Gaglioti and one anonymous reviewer who took time to carefully review this long manuscript and provide constructive comments.

Appendix A. Supplementary data

Supplementary data to this article can be found online at https://doi.org/10.1016/j.quascirev.2022.107878.

References

Abbott, M.B., Stafford, T.W., 1996. Radiocarbon geochemistry of modern and ancient Arctic lake systems, Baffin Island, Canada. Quat. Res. 45, 300–311.
Abbott, M.B., Finney, B.P., Edwards, M.E., Kelts, K.R., 2000. Lake-level reconstruction and paleohydrology of Birch Lake, central Alaska, based on seismic reflection profiles and core transects. Quat. Res. 53, 154–166.
Abbott, M.B., Edwards, M.E., Finney, B.P., 2010. A 40,000-yr record of environmental change from Burial Lake in Northwest Alaska. Quat. Res. 74, 156–165.
Ager, T.A., 2003. Late Quaternary vegetation and climate history of the central Bering land bridge from St. Michael Island, western Alaska. Quat. Res. 60, 19–32.
Alfimov, A.V., Berman, D.I., 2001. Beringian climate during the late Pleistocene and Holocene. Quat. Sci. Rev. 20, 127–134.
Anderson, R.S., 1984. Connatichela artemisiae, a new genus and species of weevil from the Yukon territory (Coleoptera: Curculionidae; leptopiinae): taxonomy, paleontology and biogeography. Can. Entomol. 116, 1571–1580.
Anderson, P.M., 1985. Late Quaternary vegetational change in the Kotzebue Sound area, northwestern Alaska. Quat. Res. 24, 307–321.
Anderson, P.M., 1988. Late quaternary pollen records from the kobuk and noatak river drainages, northwestern Alaska. Quat. Res. 29, 263–276.
Anderson, R.S., 1997. Weevils (Coleoptera: curculionoidea, excluding scolytinae and platypodinae) of the Yukon. In: Danks, H.V., Downes, J.A. (Eds.), Insects of the Yukon. Biological Survey of Canada (Terrestrial Arthropods), pp. 523–562. Ottawa.
Anderson, P.M., Edwards, M.E., Brubaker, L.B., 2003. Results and paleoclimate implications of 35 years of paleoecological research in Alaska. Dev. Quat. Sci. 1, 427–440.
Arnold, L.J., Roberts, R.G., Macphee, R.D., Haile, J.S., Brock, F., Möller, P., Froese, D.G., Tikhonov, A.N., Chivas, A.R., Gilbert, M.T.P., Willerslev, E., 2011. Paper II–Dirt, dates and DNA: OSL and radiocarbon chronologies of perennially frozen sediments in Siberia, and their implications for sedimentary ancient DNA studies. Boreas 40, 417–445.
Bartlein, P.J., Anderson, P.M., Edwards, M.E., McDowell, P.F., 1991. A framework for interpreting paleoclimatic variations in eastern Beringia. Quat. Int. 10, 73–83.
Bartlein, P.J., Edwards, M.E., Hostetler, S.W., Shafer, S.L., Anderson, P.M., Brubaker, L.B., Lozhkin, A.V., 2015. Early-Holocene warming in Beringia and its mediation by sea-level and vegetation changes. Clim. Past 11, 1197–1222.
Bartlein, P.J., Hostetler, S.W., Alder, J.R., 2014. Paleoclimate. *In Climate Change in North America* (pp. 1–51). G. Ohring (ed.), Springer International Publishing

Switzerland 2014.
Bell, K.L., De Vere, N., Keller, A., Richardson, R.T., Gous, A., Burgess, K.S., Brosi, B.J., 2016. Pollen DNA barcoding: current applications and future prospects. Genome 59, 629–640.
Berman, D.I., Korotyaev, B.A., Alfimov, A.V., 2001. Contribution to the weevil fauna (Coleoptera: apionidae, Curculionidae) of the mountain steppes in the Yukon Territory, Canada, with reference to the Pleistocene history of Beringia. Entomol. Rev. 81, 993–998 (in Russian). Translated - Zoologicheskiy Journal.
Berman, D.I., Alfimov, A.V., Kuzmina, S.A., 2011. Invertebrates of the relict steppe ecosystems of Beringia, and the reconstruction of Pleistocene landscapes. Quat. Sci. Rev. 30, 2200–2219.
Bigelow, N.H., 1997. Late Quaternary Vegetation and Lake Level Changes in Central Alaska. Unpublished PhD thesis, University of Alaska Fairbanks.
Bigelow, N.H., Edwards, M.E., 2001. A 14,000 yr paleoenvironmental record from Windmill Lake, central Alaska: lateglacial and Holocene vegetation in the Alaska range. Quat. Sci. Rev. 20, 203–215.
Bousquet, Y., Laplante, S., 2006. Coleoptera Histeridae: the Insects and Arachnids of Canada, Part 24. NRC Research Press, Ottawa.
Bright Jr., D.E., 1976. The Insects and Arachnids of Canada. Part 2. The Bark Beetles of Canada and Alaska. Coleoptera: Scolytidae. The Insects and Arachnids of Canada. Part 2. The Bark Beetles of Canada and Alaska. Coleoptera: Scolytidae. Canada Department of Agriculture, p. 241.
Bronk Ramsey, C.B., 2008. Deposition models for chronological records. Quat. Sci. Rev. 27, 42–60.
Bronk Ramsey, C.B., 2009a. Bayesian analysis of radiocarbon dates. Radiocarbon 51, 337–360.
Bronk Ramsey, C.B., 2009b. Dealing with outliers and offsets in radiocarbon dating. Radiocarbon 51, 1023–1045.
Bronk Ramsey, C.B., Lee, S., 2013. Recent and planned developments of the program OxCal. Radiocarbon 55, 720–730.
Brown, T.A., Nelson, D.E., Vogel, J.S., Southon, J.R., 1988. Improved collagen extraction by modified Longin method. Radiocarbon 30, 171–177.
Brubaker, L.B., Anderson, P.M., Edwards, M.E., Lozhkin, A.V., 2005. Beringia as a glacial refugium for boreal trees and shrubs: new perspectives from mapped pollen data. J. Biogeogr. 32, 833–848.
Buck, C.L., Barnes, B.M., 1999. Temperatures of hibernacula and changes in body composition of arctic ground squirrels over winter. J. Mammal. 80, 1264–1276.
Bunbury, J., Gajewski, K., 2009. Postglacial climates inferred from a lake at treeline, southwest Yukon Territory, Canada. Quat. Sci. Rev. 28, 354–369.
Calmels, F., Froese, D.G., 2009. Cryostratigraphic record of permafrost degradation and recovery following historic surface disturbances, Klondike area, Yukon. In: Weston, L.H., Blackburn, L.R., Lewis, L.L. (Eds.), Yukon Exploration and Geology 2008, Yukon Geological Survey, pp. 85–97.
Calmels, F., Gagnon, O., Allard, M., 2005. A portable earth-drill system for permafrost studies. Permafr. Periglac. Process. 16, 311–315.
Calmels, F., Froese, D.G., Clavano, W.R., 2012. Cryostratigraphic record of permafrost degradation and recovery following historic (1898–1992) surface disturbances in the Klondike region, central Yukon Territory. Can. J. Earth Sci. 49, 938–952.
Campbell, J.M., 1983. A revision of the North America omaliinae (Coleoptera: staphylinidae) the genus Olophrum erochson. Can. Entomol. 115, 577–622.
Clare, E.L., Economou, C.K., Faulkes, C.G., Gilbert, J.D., Bennett, F., Drinkwater, R., Littlefair, J.E., 2021. eDNAir: proof of concept that animal DNA can be collected from air sampling. PeerJ 9, e11030.
Cody, W.J., 2000. Flora of the Yukon Territory, second ed. NRC Research Press, Ottawa.
Crowson, R.A., 1981. The Biology of the Coleoptera. Academic Press, New York, p. 802.
Cwynar, L.C., 1982. A late-quaternary vegetation history from Hanging Lake, northern Yukon: ecological archives m052-001. Ecol. Monogr. 52, 1–24.
Dalton, A.S., Margold, M., Stokes, C.R., Tarasov, L., Dyke, A.S., Adams, R.S., Allard, S., Arends, H.E., Atkinson, N., Attig, J.W., Barnett, P.J., 2020. An updated radiocarbon-based ice margin chronology for the last deglaciation of the North American Ice Sheet Complex. Quat. Sci. Rev. 234, 106223.
Day, J., 1983. Manual for Describing Soils in the Field. LRRI Contribution No. 82-52. Agriculture Caanda, Ottawa.
Denton, G.H., Alley, R.B., Comer, G.C., Broecker, W.S., 2005. The role of seasonality in abrupt climate change. Quat. Sci. Rev. 24, 1159–1182.
Edwards, M.E., Brubaker, L.B., Lozhkin, A.V., Anderson, P.M., 2005. Structurally novel biomes: a response to past warming in Beringia. Ecology 86, 1696–1703.
Edwards, M.E., Alsos, I.G., Yoccoz, N., Coissac, E., Goslar, T., Gielly, L., Haile, J., Langdon, C.T., Tribsch, A., Binney, H.A., von Stedingk, H., Taberlet, P., 2018. Metabarcoding of modern soil DNA gives a highly local vegetation signal in Svalbard tundra. Holocene 28, 2006–2016.
Elias, S.A., 1994. Quaternary Insects and Their Environments. Smithsonian Institution Press, Washington, DC.
Elias, S.A., 2000. Late Pleistocene climates of Beringia, based on analysis of fossil beetles. Quat. Res. 53, 229–235.
Fisher, D., Wake, C., Kreutz, K., Yalcin, K., Steig, E., Mayewski, P., Anderson, L., Zheng, J., Rupper, S., Zdanowicz, C., Demuth, M., 2004. Stable isotope records from Mount Logan, Eclipse ice cores and nearby Jellybean Lake. Water cycle of the North Pacific over 2000 years and over five vertical kilometres: sudden shifts and tropical connections. Géogr. Phys. Quaternaire 58, 337–352.
Froese, D., Stiller, M., Heintzman, P.D., Reyes, A.V., Zazula, G.D., Soares, A.E., Meyer, M., Hall, E., Jensen, B.J., Arnold, L.J., MacPhee, R.D., 2017. Fossil and genomic evidence constrains the timing of bison arrival in North America. Proc. Natl. Acad. Sci. USA 114, 3457–3462.
Gaglioti, B.V., Mann, D.H., Wooller, M.J., Jones, B.M., Wiles, G.C., Groves, P., Kunz, M.L., Baughman, C.A., Reanier, R.E., 2017. Younger-Dryas cooling and sea-ice feedbacks were prominent features of the Pleistocene-Holocene transition in Arctic Alaska. Quat. Sci. Rev. 169, 330–343.
Gaglioti, B.V., Mann, D.H., Groves, P., Kunz, M.L., Farquharson, L.M., Reanier, R.E., Jones, B.M., Wooller, M.J., 2018. Aeolian stratigraphy describes ice-age paleoenvironments in unglaciated Arctic Alaska. Quat. Sci. Rev. 182, 175–190.
Goetcheus, V.G., Birks, H.H., 2001. Full-glacial upland tundra vegetation preserved under tephra in the Beringia national park, seward Peninsula, Alaska. Quat. Sci. Rev. 20, 135–147.
Goulet, H., 1983. The genera of Holarctic Elaphrini and species of Elaphrus Fabricius (Coleoptera: carabidae): classification, phylogeny and zoogeography. Quaest. Entomol. 19, 219–482.
Gurjeva, E.L., 1989. Family elateridae – click beetles. In: Ler, P.A. (Ed.), The Guide Book on Insects of the Far East of the USSR. v.3 (Coleoptera or Beetles), Part 1. Nauka, Leningrad, pp. 489–534 (in Russian).
Guthrie, R.D., 1982. Mammals of the mammoth steppe as paleoenvironmental indicators. In: Hopkins, D.M., Matthews, J.V., Schweger, C.E. (Eds.), Paleoecology of Beringia. Academic Press, pp. 307–326.
Guthrie, R.D., 1984. In: Martin, P.S., Klein, R.G. (Eds.), Mosaics, Allelochemics, and Nutrients: an Ecological Theory of Late Pleistocene Megafaunal Extinctions" in Quaternary Extinctions: A Prehistoric Revolution. University of Arizona Press, pp. 258–259.
Guthrie, R.D., 1990a. New dates on Alaskan Quaternary moose, Cervalces Alces - archaeological, evolutionary, and ecological implications. Curr. Res. Pleistocene 7, 111–112.
Guthrie, R.D., 1990b. Frozen Fauna of the Mammoth Steppe. University of Chicago Press.
Guthrie, R.D., 2001. Origin and causes of the mammoth steppe: a story of cloud cover, woolly mammal tooth pits, buckles, and inside-out Beringia. Quat. Sci. Rev. 20, 549–574.
Guthrie, R.D., 2006. New carbon dates link climatic change with human colonization and Pleistocene extinctions. Nature 441, 207–209.
Heintzman, P.D., Froese, D., Ives, J.W., Soares, A.E., Zazula, G.D., Letts, B., Andrews, T.D., Driver, J.C., Hall, E., Hare, P.G., Jass, C.N., MacKay, G., Southon, J.R., Stiller, M., Woywitka, R., Suchard, M.A., Shapiro, B., 2016. Bison phylogeography constrains dispersal and viability of the Ice Free Corridor in western Canada. Proc. Natl. Acad. Sci. USA 113, 8057–8063.
Higuera, P.E., Brubaker, L.B., Anderson, P.M., Brown, T.A., Kennedy, A.T., Hu, F.S., 2008. Frequent fires in ancient shrub tundra: implications of paleorecords for arctic environmental change. PLoS One 3, e0001744.
Höfle, C., Edwards, M.E., Hopkins, D.M., Mann, D.H., Ping, C.L., 2000. The full-glacial environment of the northern Seward Peninsula, Alaska, reconstructed from the 21,500-year-old Kitluk paleosol. Quat. Res. 53, 143–153.
Hopkins, D.M., 1982. Aspects of the paleogeography of Beringia during the late Pleistocene. Paleoecology of Beringia. In: Hopkins, D.M., Matthews, J.V., Schweger, C.E. (Eds.), Paleoecology of Beringia. Academic Press, pp. 307–326, 3-28.
Hu, F.S., Nelson, D.M., Clarke, G.H., Rühland, K.M., Huang, Y., Kaufman, D.S., Smol, J.P., 2006. Abrupt climatic events during the last glacial-interglacial transition in Alaska. Geophys. Res. Lett. 33.
Hultén, E., 1937. Outline of the history of arctic and boreal biota during the Quaternary period. Stockholm, Thule 168.
IAEA/WMO. Global Network of isotopes in precipitation. The GNIP database. https://nucleus.iaea.org/wiser/. Accessed 2020.
Irvine, F., Cwynar, L.C., Vermaire, J.C., Rees, A.B., 2012. Midge-inferred temperature reconstructions and vegetation change over the last~ 15,000 years from Trout Lake, northern Yukon Territory, eastern Beringia. J. Paleolimnol. 48, 133–146.
Jones, M.C., Yu, Z., 2010. Rapid deglacial and early Holocene expansion of peatlands in Alaska. Proc. Natl. Acad. Sci. USA 107, 7347–7352.
Kaufman, D.S., Axford, Y.L., Henderson, A.C., McKay, N.P., Oswald, W.W., Saenger, C., Anderson, R.S., Bailey, H.L., Clegg, B., Gajewski, K., Hu, F.S., 2016. Holocene climate changes in eastern Beringia (NW North America)—A systematic review of multi-proxy evidence. Quat. Sci. Rev. 147, 312–339.
Kokorowski, H.D., Anderson, P.M., Mock, C.J., Lozhkin, A.V., 2008. A re-evaluation and spatial analysis of evidence for a Younger Dryas climatic reversal in Beringia. Quat. Sci. Rev. 27, 1710–1722.
Kroetsch, D., Wang, C., 2008. Particle size distribution. In: Carter, M.R., Gregorich, E.G. (Eds.), Soil Sampling and Methods of Analysis, second ed. Canadian Society of Soil Science/CRC Press.
Kurek, J., Cwynar, L.C., Vermaire, J.C., 2009a. A late quaternary paleotemperature record from Hanging Lake, northern Yukon territory, eastern Beringia. Quat. Res. 72, 246–257.
Kurek, J., Cwynar, L.C., Ager, T.A., Abbott, M.B., Edwards, M.E., 2009b. Late Quaternary paleoclimate of western Alaska inferred from fossil chironomids and its relation to vegetation histories. Quat. Sci. Rev. 28, 799–811.
Kuzmina, S.A., 2017. Macroentomology analysis: methods, opportunities, and examples of reconstructions of paleoclimatic and paleoenvironmental conditions in the quaternary of the northeastern siberia. Contemporary Problems of Ecology 10 (4), 336–349.
Kuzmina, S., Sher, A., 2006. Some features of the Holocene insect faunas of northeastern Siberia. Quat. Sci. Rev. 25, 1790–1820.
Kuzmina, S., Elias, S., Matheus, P., Storer, J.E., Sher, A., 2008. Paleoenvironmental reconstruction of the last glacial maximum, inferred from insect fossils from a

buried soil at tempest lake, seward Peninsula, Alaska. Palaeogeogr. Palaeoclimatol. Palaeoecol. 267, 245–255.
Lasher, G.E., Abbott, M.B., Anderson, L., Yasarer, L., Rosenmeier, M., Finney, B.P., 2021. Holocene hydroclimatic reorganizations in northwest Canada inferred from lacustrine carbonate oxygen isotopes. Geophys. Res. Lett. 48, e2021GL092948.
Lora, J.M., Mitchell, J.L., Tripati, A.E., 2016. Abrupt reorganization of North Pacific and western North American climate during the last deglaciation. Geophys. Res. Lett. 43, 11–796.
Mackay, J.R., 1983. Downward water movement into frozen ground, western arctic coast, Canada. Can. J. Earth Sci. 20, 120–134.
Mann, D.H., Peteet, D.M., Reanier, R.E., Kunz, M.L., 2002. Responses of an arctic landscape to Lateglacial and early Holocene climatic changes: the importance of moisture. Quat. Sci. Rev. 21, 997–1021.
Mann, D.H., Groves, P., Kunz, M.L., Reanier, R.E., Gaglioti, B.V., 2013. Ice-age megafauna in Arctic Alaska: extinction, invasion, survival. Quat. Sci. Rev. 70, 91–108.
Mann, D.H., Groves, P., Reanier, R.E., Gaglioti, B.V., Kunz, M.L., Shapiro, B., 2015. Life and extinction of megafauna in the ice-age Arctic. Proc. Natl. Acad. Sci. USA 112, 14301–14306.
Martinez De La Torre, H.A., Reyes, A.V., Zazula, G.D., Froese, D.G., Jensen, B.J., Southon, J.R., 2019. Permafrost-preserved wood and bone: radiocarbon blanks from Yukon and Alaska. Nucl. Instrum. Methods Phys. Res. Sect. B Beam Interact. Mater. Atoms 455, 154–157.
Matthews, J.V., 1974. Quaternary environments at cape deceit (seward Peninsula, Alaska): evolution of a tundra ecosystem. Geol. Soc. Am. Bull. 85, 1353–1384.
Matthews, J.V., 1983. A method for comparison of northern fossil insect assemblages. Géogr. Phys. Quaternaire 37, 297–306.
Matthews, J.V., Telka, A., 1997. Insect fossils from the Yukon. In: Danks, H.V., Downes, J.A. (Eds.), Insects of the Yukon, Biological Survey of Canada (Terrestrial Arthropods), pp. 911–962. Ottawa.
McGowan, S., Anderson, N.J., Edwards, M.E., Hopla, E., Jones, V., Langdon, P.G., Law, A., Solovieva, N., Turner, S., van Hardenbroek, M., Whiteford, E.J., 2018. Vegetation transitions drive the autotrophy–heterotrophy balance in Arctic lakes. Limnology and Oceanography Letters 3, 246–255.
Meltzer, D.J., 2020. Overkill, glacial history, and the extinction of North America's Ice Age megafauna. Proc. Natl. Acad. Sci. USA 117, 28555–28563.
Meyer, H., Schirrmeister, L., Yoshikawa, K., Opel, T., Wetterich, S., Hubberten, H.W., Brown, J., 2010. Permafrost evidence for severe winter cooling during the Younger Dryas in northern Alaska. Geophys. Res. Lett. 37.
Monteath, A.J., Gaglioti, B.V., Edwards, M.E., Froese, D., 2021. Late Pleistocene shrub expansion preceded megafauna turnover and extinctions in eastern Beringia. Proc. Natl. Acad. Sci. USA 118.
Motz, J.E., Morgan, A.V., 1997. Morphological variation in Elaphrus clairvillei kirby (Coleoptera: carabidae) from fossil sites in the great lakes region. Coleopt. Bull. 51 (2), 140–145.
Murchie, T.J., Kuch, M., Duggan, A.T., Ledger, M.L., Roche, K., Klunk, J., Karpinski, E., Hackenberger, D., Sadoway, T., MacPhee, R., Froese, D., 2021a. Optimizing extraction and targeted capture of ancient environmental DNA for reconstructing past environments using the PalaeoChip Arctic-1.0 bait-set. Quat. Res. 99, 305–328.
Murchie, T.J., Monteath, A.J., Mahony, M.E., Long, G.S., Cocker, S., Sadoway, T., Karpinski, E., Zazula, G., MacPhee, R.D., Froese, D., Poinar, H.N., 2021b. Collapse of the mammoth-steppe in central Yukon as revealed by ancient environmental DNA. Nat. Commun. 12, 1–18.
Muhs, D.R., Ager, T.A., Bettis III, E.A., McGeehin, J., Been, J.M., Begét, J.E., Pavich, M.J., Stafford Jr., T.W., De Anne, S.P., 2003. Stratigraphy and palaeoclimatic significance of Late Quaternary loess–palaeosol sequences of the Last Interglacial–Glacial cycle in central Alaska. Quat. Sci. Rev. 22 (18–19), 1947–1986.
Murchie, T.J., Karpinski, E., Eaton, K., Duggan, A.T., Baleka, S., Zazula, G., MacPhee, R.D., Froese, D., Poinar, H.N., 2022. Pleistocene mitogenomes reconstructed from the environmental DNA of permafrost sediments. Curr. Biol. 32, 851–860.
Myers-Smith, I.H., Forbes, B.C., Wilmking, M., Hallinger, M., Lantz, T., Blok, D., Tape, K.D., Macias-Fauria, M., Sass-Klaassen, U., Lévesque, E., Boudreau, S., 2011. Shrub expansion in tundra ecosystems: dynamics, impacts and research priorities. Environ. Res. Lett. 6, 045509.
Nelson, R.E., Carter, L.D., 1987. Paleoenvironmental analysis of insects and extralimital Populus from an early Holocene sites on the Arctic Slope of Alaska, USA. Arct. Alp. Res. 19, 230–241.
Nielsen, M.G., 1987. The ant fauna (Hymenoptera: formicidae) in northern and interior Alaska: a survey along the trans-Alaskan pipeline and a few highways. Entomol. News 98, 74–88.
Norris, S., Tarasov, L., Monteath, A.J., Gosse, J.C., Hidy, A.J., Margold, M., Froese, D.G., 2022. Rapid Retreat of the Southwestern Laurentide Ice Sheet during the Bølling-Allerød Interval (Geology).
Pang, B.C.M., Cheung, B.K.K., 2007. One-step generation of degraded DNA by UV irradiation. Anal. Biochem. 1, 163–165.
Parducci, L., Väliranta, M., Salonen, J.S., Ronkainen, T., Matetovici, I., Fontana, S.L., Eskola, T., Sarala, P., Suyama, Y., 2015. Proxy comparison in ancient peat sediments: pollen, macrofossil and plant DNA. Phil. Trans. Biol. Sci. 370, 20130382.
Pedersen, M.W., Ginolhac, A., Orlando, L., Olsen, J., Andersen, K., Holm, J., Funder, S., Willerslev, E., Kjær, K.H., 2013. A comparative study of ancient environmental DNA to pollen and macrofossils from lake sediments reveals taxonomic overlap and additional plant taxa. Quat. Sci. Rev. 75, 161–168.
Porter, T.J., Opel, T., 2020. Recent advances in paleoclimatological studies of Arctic wedge-and pore-ice stable-water isotope records. Permafr. Periglac. Process. 31, 429–441.
Porter, T.J., Pisaric, M.F.J., Field, R., Kokelj, S.V., Edwards, T.W.D., deMontigny, P., Healy, R., LeGrande, A., 2014. Spring-summer temperatures since AD 1780 reconstructed from stable oxygen isotope ratios in white spruce tree rings from the Mackenzie Delta, northwestern Canada. Clim. Dynam. 42, 771–785.
Porter, T.J., Froese, D.G., Feakins, S.J., Bindeman, I.N., Mahony, M.E., Pautler, B.G., Reichart, G.J., Sanborn, P.T., Simpson, M.J., Weijers, J.W., 2016. Multiple water isotope proxy reconstruction of extremely low last glacial temperatures in Eastern Beringia (Western Arctic). Quat. Sci. Rev. 137, 113–125.
Porter, T.J., Schoenemann, S.W., Davies, L.J., Steig, E.J., Bandara, S., Froese, D.G., 2019. Recent summer warming in northwestern Canada exceeds the Holocene thermal maximum. Nat. Commun. 10, 1–10.
Potter, B.A., Reuther, J.D., Holliday, V.T., Holmes, C.E., Miller, D.S., Schmuck, N., 2017. Early colonization of Beringia and northern north America: chronology, routes, and adaptive strategies. Quat. Int. 444, 36–55.
Rabanus-Wallace, M.T., Wooller, M.J., Zazula, G.D., Shute, E., Jahren, A.H., Kosintsev, P., Burns, J.A., Breen, J., Llamas, B., Cooper, A., 2017. Megafaunal isotopes reveal role of increased moisture on rangeland during late Pleistocene extinctions. Nature ecology & evolution 1, 1–5.
Reimer, P.J., Austin, W.E., Bard, E., Bayliss, A., Blackwell, P.G., Ramsey, C.B., Butzin, M., Cheng, H., Edwards, R.L., Friedrich, M., Grootes, P.M., 2020. The IntCal20 Northern Hemisphere radiocarbon age calibration curve (0–55 cal kBP). Radiocarbon 62, 725–757.
Reyes, A.V., Froese, D.G., Jensen, B.J., 2010. Permafrost response to last interglacial warming: field evidence from non-glaciated Yukon and Alaska. Quat. Sci. Rev. 29, 3256–3274.
Sanborn, P.T., Smith, C.S., Froese, D.G., Zazula, G.D., Westgate, J.A., 2006. Full-glacial paleosols in perennially frozen loess sequences, Klondike goldfields, Yukon Territory, Canada. Quat. Res. 66, 147–157.
Schweger, C.E., 1982. Late Pleistocene vegetation of eastern Beringia: pollen analysis of dated alluvium. In: Hopkins, D.M., Matthews, J.V., Schweger, C.E. (Eds.), Paleoecology of Beringia. Academic Press, pp. 95–112.
Sher, A., Kuzmina, S., 2007. Beetle records/late Pleistocene of northern Asia. In: Elias, S. (Ed.), Encyclopedia of Quaternary Science 1, 246–267. Elsevier.
Skjemstad, J.O., Baldock, J.A., 2008. Total and organic carbon. Ch. 21. In: Carter, M.R., Gregorich, E.G. (Eds.), Soil Sampling and Methods of Analysis, second ed. Canadian Society of Soil Science/CRC Press, pp. 225–237.
Soil Classification Working Group, 1998. The Canadian System of Soil Classification, third ed. Agriculture and Agri-Food Canada, Ottawa, p. 187. Publ. 1646.
Stoker, B.J., Margold, M., Gosse, J.C., Hidy, A.J., Monteath, A.J., Young, J.M., Gandy, N., Gregoire, L.J., Norris, S.L., Froese, D., 2022. The collapse of the Laurentide-Cordilleran ice saddle and early opening of the Mackenzie Valley, Northwest Territories, constrained by 10Be exposure dating. Cryosphere Discuss. https://doi.org/10.5194/tc-2022-120 (in press).
Sturm, M., Racine, C., Tape, K., 2001. Increasing shrub abundance in the Arctic. Nature 411, 546–547.
Tape, K.E.N., Sturm, M., Racine, C., 2006. The evidence for shrub expansion in Northern Alaska and the Pan-Arctic. Global Change Biol. 12, 686–702.
Tinner, W., Hu, F.S., Beer, R., Kaltenrieder, P., Scheurer, B., Krähenbühl, U., 2006. Postglacial vegetational and fire history: pollen, plant macrofossil and charcoal records from two Alaskan lakes. Veg. Hist. Archaeobotany 15, 279–293.
Vershinina, A.O., Heintzman, P.D., Froese, D.G., Zazula, G., Cassatt-Johnstone, M., Dalén, L., Der Sarkissian, C., Dunn, S.G., Ermini, L., Gamba, C., Groves, P., 2021. Ancient horse genomes reveal the timing and extent of dispersals across the Bering Land Bridge. Mol. Ecol. 30, 6144–6161.
Walter, K.M., Edwards, M.E., Grosse, G., Zimov, S.A., Chapin III, F.S., 2007. Thermokarst lakes as a source of atmospheric CH4 during the last deglaciation. Science 318, 633–636.
Willerslev, E., Davison, J., Moora, M., Zobel, M., Coissac, E., Edwards, M.E., Lorenzen, E.D., Vestergård, M., Gussarova, G., Haile, J., Craine, J., 2014. Fifty thousand years of Arctic vegetation and megafaunal diet. Nature 506, 47–51.
Young, N.E., Briner, J.P., Schaefer, J., Zimmerman, S., Finkel, R.C., 2019. Early Younger Dryas glacier culmination in southern Alaska: implications for North Atlantic climate change during the last deglaciation. Geology 47, 550–554.
Zazula, G.D., Froese, D.G., Schweger, C.E., Mathewes, R.W., Beaudoin, A.B., Telka, A.M., Harington, C.R., Westgate, J.A., 2003. Ice-age steppe vegetation in east Beringia. Nature 423, 603-603.
Zazula, G.D., Froese, D.G., Westgate, J.A., La Farge, C., Mathewes, R.W., 2005. Paleoecology of beringian “packrat” middens from central Yukon territory, Canada. Quat. Res. 63, 189–198.
Zazula, G.D., Schweger, C.E., Beaudoin, A.B., McCourt, G.H., 2006. Macrofossil and pollen evidence for full-glacial steppe within an ecological mosaic along the Bluefish River, eastern Beringia. Quat. Int. 142, 2–19.
Zimov, S.A., 2005. Pleistocene park: return of the mammoth's ecosystem. Science 308, 796–798.